Pacific Northwest
NATIONAL LABORATORY

PNNL-31334 Rev 0
EWG-RPT-033 Rev 0

Glass Crystallization Constraints for WTP LAW Operations: Assessment of Isothermal Treatments on Crystal Formation

June 2021

Charmayne E Lonergan
Eden L Rivers
Suzanne M Baird
Diana L Bellafatto
Sulaiman E Sannoh
Dong-Sang Kim
John D Vienna

U.S. DEPARTMENT OF ENERGY

Prepared for the U.S. Department of Energy
under Contract DE-AC05-76RL01830

DISCLAIMER

PACIFIC NORTHWEST NATIONAL LABORATORY
operated by
BATTELLE
for the
UNITED STATES DEPARTMENT OF ENERGY
under Contract DE-AC05-76RL01830

Printed in the United States of America

Available to DOE and DOE contractors from the
Office of Scientific and Technical Information,
P.O. Box 62, Oak Ridge, TN 37831-0062;
ph: (865) 576-8401
fax: (865) 576-5728
email: reports@adonis.osti.gov

Available to the public from the National Technical Information Service
5301 Shawnee Rd., Alexandria, VA 22312
ph: (800) 553-NTIS (6847)
email: orders@ntis.gov <https://www.ntis.gov/about>
Online ordering: http://www.ntis.gov

PNNL-31334 Rev 0
EWG-RPT-033 Rev 0

Glass Crystallization Constraints for WTP LAW Operations: Assessment of Isothermal Treatments on Crystal Formation

June 2021

Charmayne E Lonergan
Eden L Rivers
Suzanne M Baird
Diana L Bellafatto
Sulaiman E Sannoh
Dong-Sang Kim
John D Vienna

Prepared for
the U.S. Department of Energy
under Contract DE-AC05-76RL01830

Pacific Northwest National Laboratory
Richland, Washington 99354

Executive Summary

Much work has been done to expand the glass composition region available for operation of the Hanford Waste Treatment and Immobilization Plant. This includes the development of updated glass property-composition models as well as constraints. This report supports this effort by suggesting constraints for avoiding excessive, and likely detrimental, crystallization during melter operation while processing advanced low-activity glass waste forms.

The constraints target SnO_2 and ZrO_2 crystals that can form when melter temperatures drop below 1100 °C. These types of crystals were found to be potentially detrimental during processing as they are denser than low-activity waste glass melts. SnO_2, density of 6.95 g/cm^3, and ZrO_2, density of 5.68 g/cm^3, have the potential to form during melter idling and settle to the bottom of the less dense glass melt (approximate density 2.65 g/cm^3). If the crystals are present in appreciable amounts, they can result in blockages of the pour-spout riser, which impacts glass pouring and melter operation. Using previously acquired results and results from testing during this effort, the following constraints (Table S.1) were determined, and are suggested as options to reduce the risk of forming crystals of the types and concentrations that are likely detrimental to melter operation.

Table S.1. Low-activity waste glass isothermal crystallization constraints.

Constraint	Limit (wt%)
SnO_2	$SnO_2 < 4.50$
ZrO_2	$ZrO_2 < 0.33 \times Na_2O + 3.70$

Acknowledgments

The authors gratefully acknowledge the financial support provided by the U.S. Department of Energy Office of River Protection Waste Treatment Plant Project managed by Tom Fletcher, with technical oversight by Albert Kruger.

The authors thank Tongan Jin for the technical review, Matt Wilburn for his editorial review, as well as David MacPherson and Veronica Perez for programmatic support during the conduct of this work.

Acronyms and Abbreviations

DOE	U.S. Department of Energy
LAW	low-activity waste
LIC	LAW isothermal crystallization
MCC	multi-component constraint
mf	mass fraction
NQAP	Nuclear Quality Assurance Program
PNNL	Pacific Northwest National Laboratory
SCC	single-component constraint
VHT	Vapor Hydration Test
VSL	Vitreous State Laboratory
WTP	Hanford Waste Treatment and Immobilization Plant
XRD	X-ray diffraction

Contents

Figures

Tables

1.0 Introduction

Operations through the Hanford Waste Treatment and Immobilization Plant (WTP) will be inextricably tied to process control models, which are the technical backbone of the integrated flowsheet. Key decisions in all unit operations rely on the ability to demonstrate that the waste feed can be effectively processed through the melter and the resulting glass product will meet disposal criteria. The demonstration of effective processing is derived from composition-property predictions and their relation to predefined acceptance criteria. In some instances, there is a lack of reasonable constraint criteria that reduces operational risks while allowing for increased waste loading, especially for crystallization constraints in processing of low-activity waste (LAW). This work contributes to the development of new crystallization constraints for the LAW.

1.1 Operational Constraints

The objective of this task was to identify at least one constraint that allows for reduced risk of operational impacts due to crystallization during LAW melter operations. This is achieved by restricting the formation of crystals that have the potential to form and settle during instances of reduced melter temperatures, e.g., temperatures near 800-1000 °C, or any temperature lower than the planned melting temperature of 1150 °C. Previous work has shown that crystals formed in the glass melt may settle and cause pouring problems due to blockages in the pour-spout riser (Matyáš et al. 2012). This settling is dependent on the crystal's density, particle size, and/or amount. This is a well-established issue in high-level waste glass melts, as spinel crystals are of great concern, but this is less well-documented in LAW glass melts.

As LAW glass formulations seek to maximize alkali loading while maintaining necessary Vapor Hydration Test (VHT) responses, cassiterite (i.e., SnO_2) is added to the melt to moderate VHT performance. It is important to note that as SnO_2 is added to help reduce VHT response, loss of SnO_2 due to crystallization also has the potential to impact waste form acceptance.

The constraints discussed in this report mainly target high-density crystals (densities greater than 5 g/cm^3) that have shown a tendency to form after isothermal heat treatments of LAW glasses. For these purposes, ZrO_2 (baddeleyite) and SnO_2 were the primary crystals of interest. Other crystals that are based on these two oxide minerals are included, but the main crystals discussed in this work are ZrO_2 and SnO_2.

The proposed constraints are single- or multi-component equations that provide a basis for effectively restricting the accessible glass compositional space for process control models based on crystal formation. The crystal constraints suggested will reduce the risk of melter damage while allowing for enhanced waste loadings. Accompanying the proposed constraints is the data that supported development of the constraints. This data originated from previous work as well as new experimental efforts that occurred as part of this task. The new experimental efforts were pursued to gain further insight into SnO_2 formation, specifically, and were designed to identify the boundary between the cassiterite formation region and homogeneous glass.

1.2 Quality Assurance

This work was performed in accordance with the Pacific Northwest National Laboratory (PNNL) Nuclear Quality Assurance Program (NQAP). The NQAP complies with DOE Order 414.1D, *Quality Assurance*, and 10 CFR 830 Subpart A, *Quality Assurance Requirements*. The NQAP uses NQA-1-2012, *Quality Assurance Requirements for Nuclear Facility Application*, as its consensus standard and NQA-1-2012, Subpart 4.2.1, as the basis for its graded approach to quality.

The NQAP works in conjunction with PNNL's laboratory-level Quality Management Program, which is based on the requirements as defined in DOE Order 414.1D, *Quality Assurance*, and 10 CFR 830, *Nuclear Safety Management*, Subpart A, *Quality Assurance Requirements*.

The work of this report was performed to the QA level of applied research with a technology readiness level of 6. This work was performed to support technology development. Data obtained may be used to support design input.

2.0 Data Compilation from Existing Literature

Existing data on LAW glasses that was subjected to isothermal heat treatments was gathered from various LAW glass reports that were previously published by PNNL (Lonergan et al. 2020; Russell et al. 2017, 2021) and the Vitreous State Laboratory (VSL) at the Catholic University of America (Matlack et al. 2001, 2006a,b, 2007a,b; Muller and Pegg 2003a-e; Muller et al. 2006; Rielley et al. 2004). Appendix A provides a summary of the database compiled with glass ID, glass composition, crystallization information, and associated report sources.

Heat treatments performed in this work and at PNNL were performed for at least 24 hours, depending on the heat treatment temperature. Heat treatments performed by VSL were performed for at least 20 hours. These data were combined into one dataset and used in constraint development to capture potential crystallization at a variety of conditions.

3.0 Experimental

This section describes how the 10 glass compositions designed to probe SnO_2 crystallization composition boundaries were established and how the associated heat treatment data was gathered. The descriptions include the matrix design for the LAW isothermal crystallization (LIC) glasses (Section 3.1), batching and melting of the 10 glasses (Section 3.2), and isothermal heat treatments that were completed on the quenched material as well as crystal phase identification and quantification for all samples via X-ray diffraction (XRD) (Section 3.3).

3.1 Matrix Design

JMP version 14.0.0 was used to design the matrix of 10 glasses covering a glass composition region based on previous work as well as adjustments to Na_2O and SnO_2 to probe the SnO_2 crystallization composition boundary. The region of interest, based on single-component constraints (SCCs), is given in Table 3.1.

Table 3.1. Single-component constraints used to define the glass composition region of interest.

SCC	Min (wt%)	Max (wt%)
Al_2O_3	3.50	15.53
B_2O_3	6.00	15.09
CaO	2.00	12.35
Cr_2O_3	0.30	1.40
Fe_2O_3	0	1.50
K_2O	0	5.90
Li_2O	0	5.86
MgO	0	10.00
Na_2O	7.50	17.50
SO_3	0.10	2.00
SiO_2	34.90	47.00
SnO_2	2.75	5.00
V_2O_5	0.50	4.00
ZnO	2.00	3.60
ZrO_2	1.00	5.03
Others	0.36	2.69

In addition to the SCCs, two multi-component constraints (MCCs), given in Table 3.2, were used.

Table 3.2. Multi-component constraints used to define the glass composition region of interest (mf = mass fraction).

MCC	Lower	Upper
$Na_2O + 0.66K_2O + 2.07Li_2O$ (mf)	0.150	0.265
Viscosity (η_{1150} °C, Pa.s)	1	10

The JMP design of experiments mixture feature was used to generate five space-filling matrices whose composition bounds were defined according to the constraints given in Table 3.1 and Table 3.2. The options applied in the JMP routine include a mixture design with the Fast Flexible Filling optimality criterion of “MaxPro” with a matrix of individual glass compositions specified. The random number generator seed value was chosen arbitrarily.

To select one matrix of 10 glasses, the dispersion and the relative range for each matrix were calculated and compared. The dispersion value was required to be less than 1.0 and the relative range greater than or equal to 0.85. The final compositions for the matrix of choice are given in Table 3.3.

Table 3.3. Glass IDs and compositions, in mf, for the 10 matrix glasses.

	LIC-01	LIC-02	LIC-03	LIC-04	LIC-05	LIC-06	LIC-07	LIC-08	LIC-09	LIC-10
Al_2O_3	0.14616	0.14904	0.03531	0.06006	0.09065	0.06879	0.05059	0.06514	0.14120	0.08398
B_2O_3	0.06558	0.07468	0.13598	0.06666	0.14113	0.12052	0.14012	0.06068	0.11101	0.08645
CaO	0.10384	0.02516	0.05133	0.03181	0.02873	0.05441	0.07547	0.02266	0.03313	0.11754
Cr_2O_3	0.00507	0.01355	0.01064	0.01197	0.00543	0.00753	0.00312	0.00425	0.00675	0.01330
Fe_2O_3	0.00583	0.01019	0.00004	0.00211	0.00512	0.00672	0.01337	0.00841	0.01387	0.00804
K_2O	0.00428	0.02852	0.00626	0.03442	0.05642	0.04584	0.03304	0.01077	0.01218	0.05305
Li_2O	0.05443	0.05841	0.03288	0.01669	0.00160	0.03065	0.00974	0.01405	0.04758	0.03403
MgO	0.07983	0.00096	0.00635	0.08273	0.04869	0.01020	0.01360	0.09985	0.04027	0.00936
Na_2O	0.07653	0.11650	0.16930	0.09466	0.13243	0.07963	0.11831	0.15462	0.09223	0.10524
SO_3	0.00685	0.01877	0.00599	0.01197	0.00220	0.01498	0.01099	0.01603	0.00559	0.00196
SiO_2	0.34906	0.35092	0.40723	0.46427	0.35044	0.44683	0.38982	0.41667	0.35977	0.35992
SnO_2	0.02908	0.03189	0.03342	0.03798	0.04754	0.04460	0.03732	0.03003	0.04405	0.02795
V_2O_5	0.01586	0.02524	0.03708	0.03210	0.02983	0.01050	0.02206	0.00672	0.00844	0.00506
ZnO	0.02366	0.03598	0.03418	0.03057	0.02872	0.02000	0.02218	0.02566	0.03273	0.02437
ZrO_2	0.01592	0.04972	0.01285	0.01191	0.01022	0.02007	0.03516	0.04102	0.04721	0.04410
$Cl^{(a)}$	0.00312	0.00181	0.00367	0.00175	0.00362	0.00325	0.00436	0.00406	0.00069	0.00445
$F^{(a)}$	0.00474	0.00275	0.00557	0.00266	0.00549	0.00493	0.00661	0.00617	0.00105	0.00676
$P_2O_5{}^{(a)}$	0.01015	0.00589	0.01192	0.00569	0.01175	0.01056	0.01415	0.01320	0.00225	0.01445

(a) Indicates the “Others” components, i.e., Cl, F, and P_2O_5.

3.2 Glass Preparation

The glasses were designed according to the steps specified in Section 3.1. Once designed, the glasses were batched using oxides, carbonates, sodium chloride, sodium fluoride, sodium sulfate, and sodium phosphate. The chemicals were mixed together in the appropriate concentrations and homogenized using an Angstrom vibratory mill with an agate mill chamber. The 10 glasses were prepared in batches of 450 g and melted at 1150 °C for 1 h, with the exception of LIC-01, whose temperature was increased after an hour to 1250 °C for 0.5 h. After the first melt was completed, the glasses were ground in a tungsten carbide mill chamber and remelted. The quantity of remelts as well as the chosen temperatures were determined by the glass response upon quenching. Glasses with crystals present upon quenching had an increase in melt temperature for the subsequent melts. Table 3.4 summarizes the melt history of the glasses. Multiple temperatures and times are shown if the temperature was increased during the melt.

Table 3.4. Melt history for 10 matrix glasses.

	1st Melt		2nd Melt		3rd Melt		4th Melt	
Glass ID	Temperature (°C)	Time (h)	Temperature (°C)	Time (h)	Temperature (°C)	Time (h)	Temperature (°C)	Time (h)
LIC-01	1150/1250	1/0.5	1200	1	1200	2	1350/1500	1/1.3
LIC-02	1200	1	1200	1	1200	1	1350/1500	1/1.3
LIC-03	1200	1	1200	1	1200	1	NA	NA
LIC-04	1150	1	1150	1	1200	1	1350	1.3
LIC-05	1150	1	1150	1	1200	1	1350	1
LIC-06	1150	1	1200	1	1200	1	1350	1
LIC-07	1150	1	1150	1	1200	1	NA	NA
LIC-08	1150	1	1200	2	1250	2.3	1350	1
LIC-09	1150/1250	1/1	1350	1	1500	1	1500	1
LIC-10	1150	1	1250	1	1350	1	NA	NA

Images of the quenched glasses after their final melts are shown in Appendix B. Some glasses (LIC-02, LIC-04, and LIC-09) required three or four melts and still did not achieve a homogeneous glass. The modified glasses are discussed in Sections 3.2.1, 3.2.2, and 3.2.3.

3.2.1 LIC-02 Modification

LIC-02 was melted four times and had a sulfate layer and phase separation throughout the various melts. Images of the first melt at 1200 °C and the final melt at 1500 °C are shown in Figure 3.1.

Figure 3.1. Images of LIC-02 after the first melt at 1200 °C (left) and the fourth and final melt at 1500 °C (right).

The first modification of the glass (i.e., LIC-02_mod1) had a decrease in the SO_3 and ZrO_2 concentrations, by 0.3 and 0.9 wt%, respectively, with an equal increase in the SiO_2 concentration (i.e., by 1.2 wt%). These composition changes did not make the glass homogeneous after melting and therefore another modification was pursued. Modification #2, LIC-02_mod2, decreased the amount of Al_2O_3 by 1 wt% and increased "Others" by the same amount relative to the first modification. The glass components that were not varied were kept at their initial concentrations. A summary of composition changes is given in Table 3.5.

Table 3.5. Concentrations for components varied for modifications of LIC-02.

Component Varied	Concentration in LIC-02 (wt%)	Concentration in LIC-02_mod1 (wt%)	Concentration in LIC-02_mod2 (wt%)
Al_2O_3	14.90	14.90	13.90
SO_3	1.88	1.58	1.58
ZrO_2	4.97	4.07	4.07
Others	1.05	1.05	2.05
All other components	See Table 3.3	No change	No change

The final modification (i.e., LIC-02_mod2) did not form a homogeneous melt, as can be seen in Figure 3.2.

Figure 3.2. LIC-02_mod2 quenched glass after third melt at 1500 °C for 1 hour.

The LIC-02 glass, and the associated modifications, were not used in determining the crystallization constraints discussed in this work.

3.2.2 LIC-04 Modification

LIC-04 was melted four times and was inhomogeneous with excess sulfate as well as phase separation visible upon quenching. Images of the first melt at 1150 °C and the fourth/final melt at 1350 °C are shown in Figure 3.3.

Figure 3.3. LIC-04 after the first melt at 1150 °C (left) and the fourth melt at 1350 °C (right).

Only one modification was made for LIC-04: Na_2O was increased by 5 wt% while SiO_2 was decreased by the same amount. All other components remained the same. Table 3.6 provides a summary of the changes.

Table 3.6. Concentrations for components varied for modification of LIC-04.

Component Varied	Concentration in LIC-04 (wt%)	Concentration in LIC-04_mod1 (wt%)
Na_2O	9.47	14.47
SiO_2	46.43	41.43
All other components	See Table 3.3	No change

The modification to LIC-04 worked well to generate a homogeneous glass; Figure 3.4 shows a photo of the modified quenched glass after the third melt at 1500 °C. LIC-04_mod1 was used for further isothermal constraint development.

Figure 3.4. LIC-04_mod1 quenched glass after third melt at 1500 °C for 1 hour.

3.2.3 LIC-09 Modification

LIC-09 was melted four times, and while improvements in homogeneity were noted with each melt, the final quenched glass was still phase separated. The first and fourth melts are shown in Figure 3.5.

Figure 3.5. LIC-09 first melt at 1150 °C (left) and fourth/final melt at 1500 °C (right).

Several modifications were attempted for LIC-09. For the first modification (i.e., LIC-09_mod1), ZrO_2 was decreased by 0.5 wt% and the "Others" component was increased by the same. In the second modification, SiO_2 was increased by 2 wt%, ZnO decreased by 0.5 wt%, SnO_2 decreased by 0.25 wt%, and Al_2O_3 decreased by 1.25 wt%. LIC-09_mod3 maintained the composition changes of mod2 while further decreasing ZrO_2 by 1 wt% and increasing "Others" by 1 wt%. Table 3.7 provides a summary of changes.

Table 3.7. Concentrations for components varied for modifications of LIC-09.

Component Varied	Concentration in LIC-09 (wt%)	Concentration in LIC-09_mod1 (wt%)	Concentration in LIC-09_mod2 (wt%)	Concentration in LIC-09_mod3 (wt%)
Al_2O_3	14.12	14.12	12.87	12.87
SiO_2	35.98	35.98	37.98	37.98
SnO_2	4.41	4.41	4.16	4.16
ZrO_2	4.72	4.22	4.22	3.22
Others	0.40	0.90	0.90	1.90
All other components	See Table 3.3	No change	No change	No change

The final modification, LIC-09_mod3, worked well to produce a homogeneous glass. The crucible and the final quenched glass are shown in Figure 3.6. The final, modified glass was used in the generation of the isothermal crystallization constraints discussed in this work.

Figure 3.6. LIC-09_mod3 final melt crucible (left) and quenched glass (right) after pouring from 1450 °C.

3.3 Isothermal Heat Treatments

Equilibrium crystal fraction at a fixed temperature was measured in Pt-10%Rh crucibles and boats with tight-fitting lids (to minimize volatility) according to the ASTM International standard procedure *Standard Test Method for Determining Liquidus Temperature of Immobilized Waste Glasses and Simulated Waste Glasses* (ASTM C1720). The primary heat treatment times and temperatures were 24 ± 0.5 h at 950 °C, 48 ± 1 h at 850 °C, and 72 ± 2 h at 750 °C, with the times chosen to improve the chances of achieving equilibrium without excessive volatility. Some glasses were tested at other temperatures as well if crystals did not form at the main three temperatures chosen. The samples were then quenched and XRD was performed.

The phases and amounts of crystals formed during heat treatment were analyzed by XRD according to Section 12.4.4 of ASTM C1720. Powdered glass samples were prepared using 5-wt% CeO_2 as an internal standard phase with between 1.5 and 2.5 g of glass powder. Glass and CeO_2 were milled together for 2 min in a 10-cm^3 tungsten carbide disc mill. The powdered samples were loaded into XRD sample holders and scanned at a 0.04° 2θ step size, 4-s dwell time, from 10° to 70° 2θ scan range. XRD spectra were analyzed with TOPAS 4.2 software (Bruker AXS Inc., Madison, Wisconsin) for phase identification and Rietveld refinement to semi-quantify the amounts of crystal phases in some samples with high crystalline content. These results are discussed in Section 4.1.

4.0 Results and Discussion

This section provides the resulting heat treatment data from the nine original glasses tested in this effort as well as the SnO_2 and ZrO_2 constraints designed from the LAW data shown in Appendix A. This compiled data included the heat treatment data shown below. The majority of the crystallization information from the LAW glass literature was presented in vol%; therefore, the constraint development uses vol% for representing the amount of crystals present. The conversion from wt% to vol% was completed using the following equation:

$$vol\%_{crystal} = \frac{\rho_{glass}}{\left(\rho_{crystal} \times \left(100 \div wt\%_{crystal}\right) + \rho_{crystal}\right)} \times 100 \quad 4.1$$

where the $vol\%_{crystal}$ = the amount of crystal present in volume percent, $wt\%_{crystal}$ = the amount of crystal present in weight percent, ρ_{glass} = glass density (2.65 g/cm^3), and $\rho_{crystal}$ = crystal density (either 6.95 g/cm^3 for SnO_2 or 5.96 g/cm^3 for ZrO_2). This conversion assumed that the residual glass density is always 2.65 g/cm^3.

4.1 Results for LIC Glasses

The statistically designed glasses were treated as described in Section 3.3 and analyzed after heating to determine the types and amounts of crystals. Table 4.1 provides a summary of the total crystal concentrations, in wt%, and the major phases present, along with the SnO_2 amount, for 750, 850, and 950 °C. Optical images of the samples and XRD data are provided in Appendix C and Appendix D, respectively. Phases presented below indicate best fit possible; certain phases may be unlikely [e.g., a $Li_2Fe_3SbO_8$ phase] but provide space group and cell parameter information. Additionally, totals may vary slightly from sums of phases due to rounding.

Table 4.1. Amount of crystals and phases of crystals, with corresponding amounts, for the LIC matrix glasses. Totals may vary slightly due to rounding.

	750 °C (72 h)		850 °C (48 h)		950 °C (72 h)	
Glass ID	Total Amount (wt%)	Phases (amounts wt%)	Total Amount (wt%)	Phases (amounts wt%)	Total Amount (wt%)	Phases (amounts wt%)
LIC-01	48.15	Diopside (26.29); Nepheline (10.80); Cassiterite (2.44); and 3 others	46.71	Diopside (21.55); Nepheline (7.72); Cassiterite (0.69); and 3 others	9.87	Forsterite (6.28); Hedenbergite (2.06); Cassiterite (1.07); $Li_2Fe_3SbO_8$ (0.46)
LIC-03	0.00	None	0.00	None	0.00	None
LIC-04_mod1	3.07	Diopside (2.38); $Li_2Fe_3SbO_8$ (0.69)	3.32	Diopside (2.75); $Li_2Fe_3SbO_8$ (0.57)	3.02	Cassiterite (1.72); $Li_{0.5}Fe_{2.5}O_4$ (0.67); $Li_2Fe_3SbO_8$ (0.63)
LIC-05	0.00	None	0.30	Cassiterite (0.30)	2.55	Cassiterite (2.55)
LIC-06	0.00	None	0.00	None	0.24	Cassiterite (0.24)
LIC-07	0.68	Baddeleyite (0.68)	1.27	Baddeleyite (1.27)	0.00	None
LIC-08	4.61	Diopside (3.35); Forsterite (1.26)	1.18	Forsterite (1.18)	1.91	Forsterite (1.33); Cassiterite (0.58)
LIC-09_mod3	4.52	Diopside (1.08); Cassiterite (1.05); Forsterite (0.84); and 3 others	3.95	Cassiterite (2.66); Magnesioferrite (0.48); $Li_2Fe_3SbO_8$ (0.40); and 2 others	4.23	Cassiterite (2.96); Magnesioferrite (1.27)
LIC-10	1.50	Baddeleyite (1.50)	0.09	$Li_2Fe_3SbO_8$ (0.09)	0.36	Cassiterite (0.22); $Li_2Fe_3SbO_8$ (0.13)

Only one glass, LIC-03, showed no crystallization at any heat treatment temperature. LIC-06 was another glass very little crystallization, precipitating 0.05 wt% SnO_2 only at 950 °C after 24 h. Overall, all glasses except for LIC-03 had SnO_2 form after at least one heat treatment, which resulted in a successful matrix design effort. The goal of the LIC glass matrix was to gather additional information about SnO_2 formation, and this was achieved. As there were multiple temperatures for heat treatments, the maximum SnO_2 amount formed at a given temperature was used in the constraint design. Many crystals other than baddeleyite and cassiterite formed in these glasses. It should be considered if other constraints would be necessary for WTP operations.

4.2 SnO_2 Constraint

The minimum and maximum amounts of SnO_2 present in the LAW glasses were 0 vol% and 1.5 vol%, respectively, according to the data compiled. The constraint for restricting the formation of SnO_2 was designed by looking at the relationship between the maximum cassiterite formation for a given glass at any heat treatment temperature and the SnO_2 amount in the associated target glass composition. The graph is shown below, Figure 4.1. A boundary region was identified after noting the clustering of data in the bottom right of the plot, as if a right triangle.

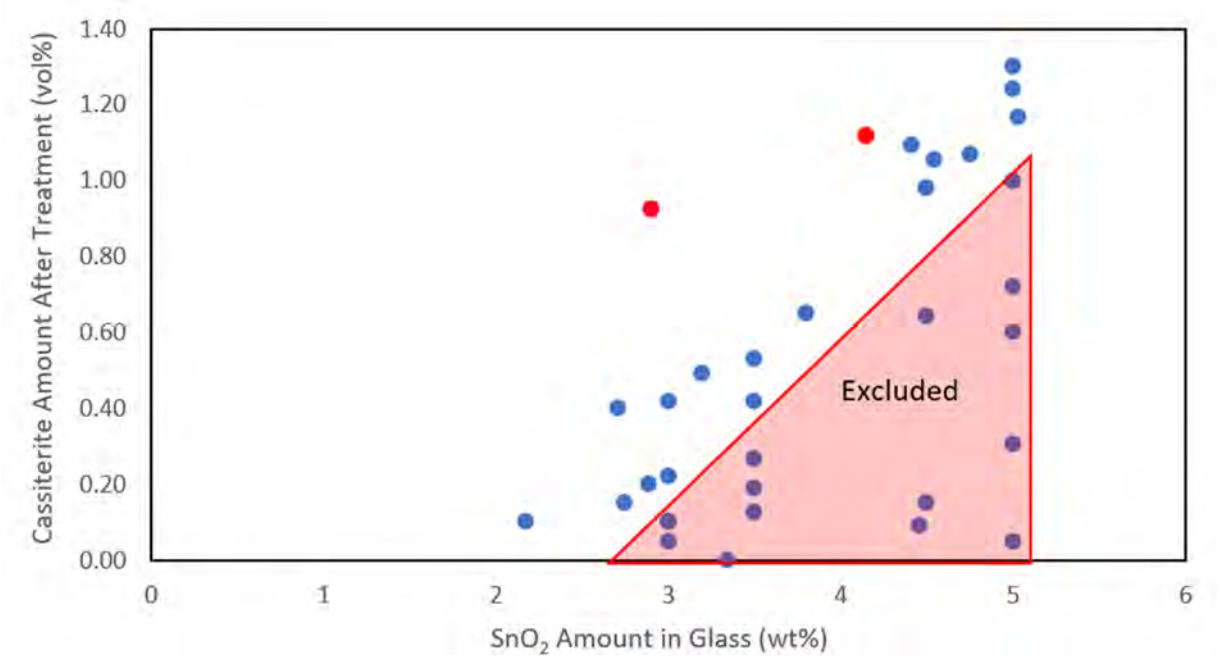

Figure 4.1. SnO_2 amount in glass plotted as a function of cassiterite formation after heat treatment.

Excluding the data points shown in red and covered by the red triangle, the boundary region was defined by a linear fit shown in Figure 4.2 with the remaining data points.

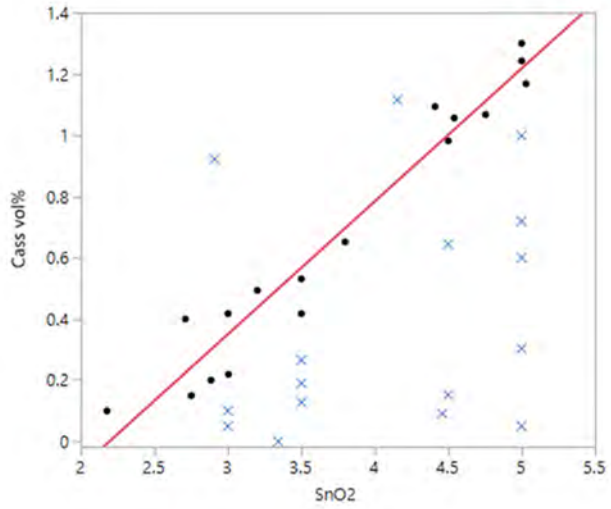

Figure 4.1. SnO_2 amount (wt%) in glass as a function of cassiterite amount precipitated after heat treatment.

The resulting equation for the red line in Figure 4.2 is:

$$cassiterite\ (vol\%) = -0.951145 + 0.4338521\ x\ SnO_2(wt\%) \quad 4.1$$

When the equation is used to determine the maximum amount of SnO_2 that is allowable for a 1 vol% cassiterite limit, as employed in other crystal constraints (Kot et al. 2001; Piepel et al. 2008; Vienna et al. 2014), the limit for SnO_2 in glass is 4.50 wt%. Tables summarizing the data used may be found in Appendix A.

The suggested constraint, which restricts the amount of SnO_2 in the glass is the following equation.

$$SnO_2 < 4.50\ (wt\%) \quad 4.2$$

4.3 ZrO_2 Constraint

The constraint for restricting ZrO_2 formation in LAW glasses was designed based on limiting ZrO_2 crystallization to less than 1.0 vol% according to crystal formation for any isothermal heat treatment below 1100 °C. The minimum and maximum amounts of ZrO_2 that formed in the glasses after treatment were 0.06 vol% and 3.0 vol%, respectively. The plotted data (**Error! Reference source not found.**) can be seen in with the maximum ZrO_2 concentration formed at any heat treatment temperature in the glass as a function of the Na_2O concentrations are shown below with the resulting ZrO_2 constraint.

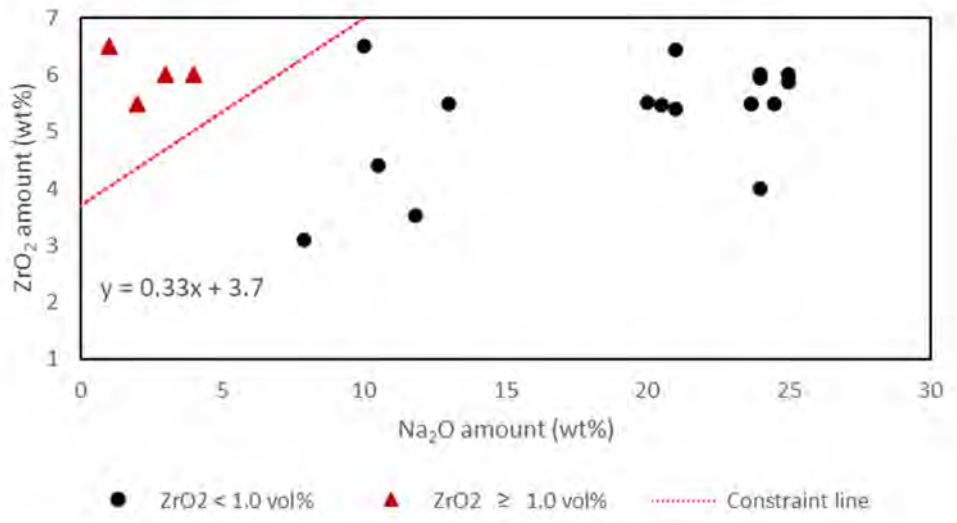

Figure 4.3. ZrO_2 amount versus Na_2O amount for glasses that contained ZrO_2 crystals.

The suggested ZrO_2 constraint, shown as the red dotted line, is:

$$ZrO_2 < 0.33 \times Na_2O + 3.70\ (wt\%) \quad 4.3$$

As there is a large empty region between the two sets of data (< 1.0 vol% and ≥ 1.0 vol%) further work may be done to refine this constraint.

5.0 Summary

Crystallization data from various LAW glass reports was compiled to determine crystallization constraints. These constraints were pursued as ways to mitigate crystal formation that might be detrimental to WTP LAW vitrification operations. Primary crystals of concern were SnO_2 and ZrO_2, as these crystals are frequently formed and have densities of 5 g/cm^3 or above. Also, their addition to glass serves the role of improving glass durability, which may not happen if they crystallize out of the glass. After a preliminary assessment of compiled data, 10 glasses were designed to crystallize SnO_2 upon isothermal heat treatments. Of the 10 glasses designed in this effort, only one (LIC-03) did not precipitate SnO_2 after any heat treatment. One glass (LIC-02) was modified twice but did not produce a homogeneous glass upon quenching.

The constraints resulting from this effort are proposed to restrict the amount of ZrO_2 and SnO_2 that may form during melter operation to less than approximately 1.0 vol% for either crystal. The suggested constraints, given in Table 5.1, will allow for less risk when processing enhanced waste glass formulations while allowing for access to higher waste loadings for LAW glasses.

Table 5.1. Low-activity waste glass isothermal crystallization constraints.

Constraint	Limit (wt%)
SnO_2	$SnO_2 < 4.50$
ZrO_2	$ZrO_2 < 0.33 \times Na_2O + 3.70$

6.0 References

10 CFR 830 Subpart A, *Quality Assurance Requirements*. U.S. Code of Federal Regulations.

ASTM C1720, *Standard Test Method for Determining Liquidus Temperature of Immobilized Waste Glasses and Simulated Waste Glasses.* ASTM International, West Conshohocken, PA.

DOE Order 414.1D, *Quality Assurance.* U.S. Department of Energy, Washington, DC.

Kot WK and IL Pegg. 2001. *Glass Formulation and Testing with RPP-WTP HLW Simulants*. VSL-01R2540-2, Vitreous State Laboratory, The Catholic University of America, Washington, DC.

Lonergan CE, JL George, D Cutforth, T Jin, P Cholsaipant, SE Sannoh, CH Skidmore, BA Stanfill, SK Cooley, RL Russell, and JD Vienna. 2020. *Enhanced Hanford Low-Activity Waste Glass Property Data Development: Phase 3*. PNNL-29847, Pacific Northwest National Laboratory, Richland, WA.

Matlack KS, I Joseph, W Gong, IS Muller, and IL Pegg. 2007a. *Enhanced LAW Glass Formulation Testing*. VSL-07R1130-1, Vitreous State Laboratory, The Catholic University of America, Washington, DC.

Matlack KS, IS Muller, W Gong, and IL Pegg. 2006a. *DuraMelter 100 Tests To Support LAW Glass Formulation Correlation Development.* VSL-06R6480-1, Vitreous State Laboratory, The Catholic University of America, Washington, DC.

Matlack KS, IS Muller, W Gong, and IL Pegg. 2007b. *Small Scale Melter Testing of LAW Salt Phase Separation*. VSL-07R7480-1, Rev. 0, Vitreous State Laboratory, The Catholic University of America, Washington, DC.

Matlack KS, S Morgan, and IL Pegg. 2001. *Melter Tests with LAW Envelope A and C Simulants To Support Enhanced Sulfate Incorporation.* VSL-01R3501-2, Rev. 0, Vitreous State Laboratory, The Catholic University of America, Washington, DC.

Matlack KS, W Gong, IS Muller, I Joseph, and IL Pegg. 2006b. *LAW Envelope A and B Glass Formulations Testing To Increase Waste Loading*. VSL-06R6900-1, Rev. 0, Vitreous State Laboratory, The Catholic University of America, Washington, DC.

Matyas, J, AR Huckleberry, CP Rodriguez, JB Lang, AT Owen, and AA Kruger. 2012. *HLW Glass Studies: Development of Crystal-Tolerant HLW Glasses.* PNNL-21308, Pacific Northwest National Laboratory, Richland, WA.

Muller IS and IL Pegg. 2003a. *Baseline LAW Glass Formulation Testing*. VSL-03R3460-1, Vitreous State Laboratory, The Catholic University of America, Washington, DC.

Muller IS and IL Pegg. 2003b. *LAW Glass Formulation To Support Melter Runs with Simulants*. , VSL-03R3460-2, Vitreous State Laboratory, The Catholic University of America, Washington, DC.

Muller IS and IL Pegg. 2003c. *LAW Glass Formulation To Support AZ-102 Actual Waste Testing*. VSL-03R3470-1, Rev.0, Vitreous State Laboratory, The Catholic University of America, Washington, DC.

Muller IS and IL Pegg. 2003d. *LAW Glass Formulation To Support AZ-101 Actual Waste Testing*. VSL-03R3470-3, Vitreous State Laboratory, The Catholic University of America, Washington, DC.

Muller IS and IL Pegg. 2003e. *LAW Glass Formulation To Support AP-101 Actual Waste Testing*. VSL-03R3470-2, Vitreous State Laboratory, The Catholic University of America, Washington, DC .

Muller IS, I Joseph, and IL Pegg. 2006. *Preparation and Testing of Law High Phosphorus and High-Chromium Glasses*. VSL-06R6480-2, Rev. 0, Vitreous State Laboratory, The Catholic University of America, Washington, DC.

NQA-1-2012, *Quality Assurance Requirements for Nuclear Facility Application*. American Society of Mechanical Engineers, New York, NY.

Piepel GF, SK Cooley, A Heredia-Langner, SM Landmesser, WK Kot, H Gan, and IL Pegg. 2008. *IHLW PCT, Spinel T1%, Electrical Conductivity, and Viscosity Model Development*. VSL-07R1240-4, Rev.0, Vitreous State Laboratory, The Catholic University of America, Washington, DC.

Rielley E, IS Muller, and IL Pegg. 2004. *Preparation and Testing of LAW Matrix Glasses To Support WTP Property-Composition Model Development*. VSL-04R4480-1, Rev.0, Vitreous State Laboratory, The Catholic University of America, Washington, DC.

Russell RL, BP McCarthy, SK Cooley, EA Cordova, SE Sannoh, V Gervasio, MJ Schweiger, JB Lang, CH Skidmore, CE Lonergan, BA Stanfill, JM Meline, and JD Vienna. 2021. *Enhanced Hanford Low-Activity Waste Glass Property Data Development: Phase 2*. PNNL-28838, Rev. 2, Pacific Northwest National Laboratory, Richland, WA.

Russell RL, T Jin, BP McCarthy, LP Darnell, DE Rinehart, CC Bonham, V Gervasio, JM Mayer, CL Arendt, JB Lang, MJ Schweiger, and JD Vienna. 2017. *Enhanced Hanford Low-Activity Waste Glass Property Data Development: Phase 1*. PNNL-26630, Pacific Northwest National Laboratory, Richland, WA.

Appendix A – Summary of Data Used in Constraint Development

This appendix contains the glass IDs, sources, compositions, and crystallization information for glasses considered in the development of the crystallization constraints discussed in this report.

Table A.1. Glass IDs, sources, and compositions for glasses considered in the development of the SnO_2-based constraint.

Source	Glass ID	Al_2O_3	B_2O_3	CaO	Cr_2O_3	Fe_2O_3	K_2O	Li_2O	Na_2O	SO_3	SiO_2	SnO_2	ZnO	ZrO_2	Others
PNNL-26630	New-IL-5253	6.25	11.75	2.75	0.08	1.25	0.20	3.50	15.00	1.30	39.75	3.50	4.00	4.50	6.18
PNNL-26630	New-IL-5255	6.25	11.75	2.75	0.08	1.25	0.20	3.50	18.00	1.30	36.75	3.50	4.00	4.50	6.18
PNNL-26630	New-IL-94020	11.50	8.00	3.53	0.08	1.25	0.20	3.50	15.00	1.02	43.25	3.50	4.00	1.50	3.68
PNNL-26630	New-IL-166697	11.25	10.22	2.75	0.21	1.25	1.00	3.50	17.49	1.29	36.75	3.50	4.00	1.50	5.29
PNNL-26630	New-IL-166731	11.50	9.31	2.75	0.21	0.50	0.20	3.50	18.02	1.27	36.75	3.20	4.00	1.50	7.29
PNNL-26630	New-OL-45748	13.85	6.00	12.24	0.31	1.50	0.00	5.00	11.40	0.10	34.00	5.00	5.00	0.00	5.60
PNNL-26630	New-OL-54017	3.50	6.00	11.17	0.04	1.50	0.00	0.00	15.00	0.10	47.00	5.00	5.00	0.00	5.70
PNNL-26630	New-OL-62380	3.50	13.75	12.24	0.08	1.50	1.50	0.00	14.01	0.10	34.00	4.50	5.00	6.50	3.31
PNNL-26630	New-OL-65959Mod	13.85	13.05	0.00	0.04	0.00	0.00	5.00	16.50	0.10	34.50	4.50	5.00	0.00	7.45
PNNL-26630	New-OL-80309	3.50	13.75	0.00	0.04	1.50	1.50	5.00	15.10	1.75	34.00	4.50	5.00	6.50	7.85
PNNL-26630	New-OL-90780	13.85	13.75	0.00	0.31	0.00	1.50	5.00	15.51	1.64	34.25	3.00	1.00	0.00	10.19
PNNL-26630	New-OL-127708Mod	10.94	13.75	0.30	0.04	1.50	1.50	2.01	12.50	0.61	47.00	5.00	1.00	0.00	3.85
PNNL-26630	New-OL-116208Mod	3.53	6.05	12.35	0.31	1.51	0.00	5.05	16.34	0.93	34.31	4.54	1.01	6.56	7.50
PNNL-26630	New-OL-108249Mod	12.03	6.04	10.07	0.31	1.51	1.51	5.03	15.61	0.89	34.23	5.03	5.03	0.00	2.70
PNNL-28838 Rev 2	LP2-OL-18	6.00	6.00	8.72	0.60	0.00	0.00	0.00	21.00	1.14	34.90	3.50	3.60	6.50	8.04
VSL-18R4360-1, Rev. 0	LORPM3S4-W	4.20	7.30	1.80	0.30	7.20	1.00	0.00	22.90	4.00	37.30	5.00	1.70	1.60	9.45
VSL-18R4360-1, Rev. 0	LORPM5S4-W	10.90	6.10	4.30	0.30	8.10	0.60	5.00	8.40	4.00	48.50	5.00	1.00	0.00	1.68
VSL-18R4360-1, Rev. 0	LORPM6S4-W	3.50	13.70	12.30	0.30	0.30	0.80	0.00	13.20	4.00	35.00	5.00	5.00	5.10	5.78
VSL-18R4360-1, Rev. 0	LORPM15S4-W	5.60	7.60	5.90	0.10	6.50	1.30	4.00	10.10	4.00	40.60	3.60	1.80	5.00	7.85

Source	Glass ID	Al_2O_3	B_2O_3	CaO	Cr_2O_3	Fe_2O_3	K_2O	Li_2O	Na_2O	SO_3	SiO_2	SnO_2	ZnO	ZrO_2	Others
VSL-18R4360-1, Rev. 0	LORPM16R1S4-W	11.80	12.30	2.50	0.30	2.60	2.50	4.00	10.70	4.00	38.60	2.90	4.00	2.30	5.38
VSL-18R4360-1, Rev. 0	LORPM18S4	5.60	7.60	2.50	0.00	1.80	1.30	3.40	10.60	4.00	48.00	4.00	1.80	4.60	8.81
VSL-18R4360-1, Rev. 0	LORPM26S4-W	10.10	6.10	10.10	0.30	7.30	5.40	0.00	11.00	4.00	35.30	5.00	5.00	0.00	4.28
VSL-18R4360-1, Rev. 0	LORPM29S4-W	9.50	10.00	0.00	0.30	0.30	5.90	5.10	8.90	4.00	35.40	5.10	4.60	5.50	9.38
VSL-18R4360-1, Rev. 0	LORPM30S4	3.50	6.00	12.30	0.10	8.00	5.90	4.40	5.00	4.00	35.00	5.00	1.00	6.00	7.88
VSL-09R1510-2, Rev. 0	ORPLA25	9.17	8.39	3.45	0.49	0.00	0.58	0.00	26.00	0.20	39.10	3.00	2.89	6.00	0.73
VSL-14R3050-1, Rev. 0	LORPM23	12.61	7.07	1.81	0.01	6.86	0.11	5.00	8.81	0.10	36.69	2.88	1.00	6.00	11.05
VSL-14R3050-1, Rev. 0	LORPM24	11.38	6.00	0.00	0.01	7.10	5.88	0.00	13.48	0.28	35.98	2.18	4.57	5.25	7.90
VSL-14R3050-1, Rev. 0	LORPM26	10.05	6.00	10.04	0.32	7.20	5.31	0.00	10.92	0.91	35.00	5.00	5.00	0.00	4.26
VSL-14R3050-1, Rev. 0	LORPM29	9.39	9.92	0.00	0.32	0.30	5.88	5.00	8.86	1.00	35.00	5.00	4.60	5.42	9.32
VSL-14R3050-1, Rev. 0	LORPM31	10.94	10.13	0.00	0.32	6.38	0.11	4.35	9.46	1.00	35.00	5.00	5.00	6.00	6.31
Current study	LIC-01	14.62	6.56	10.38	0.51	0.58	0.43	5.44	7.65	0.69	34.91	2.91	2.37	1.59	11.37
Current study	LIC-03	3.53	13.60	5.13	1.06	0.00	0.63	3.29	16.93	0.60	40.72	3.34	3.42	1.29	6.46
Current study	LIC-04_mod1	6.01	6.67	3.18	1.20	0.21	3.44	1.67	14.47	1.20	41.43	3.80	3.06	1.19	12.49
Current study	LIC-05	9.06	14.11	2.87	0.54	0.51	5.64	0.16	13.24	0.22	35.04	4.75	2.87	1.02	9.94
Current study	LIC-06	6.88	12.05	5.44	0.75	0.67	4.58	3.06	7.96	1.50	44.68	4.46	2.00	2.01	3.94
Current study	LIC-07	5.06	14.01	7.55	0.31	1.34	3.30	0.97	11.83	1.10	38.98	3.73	2.22	3.52	6.08
Current study	LIC-08	6.51	6.07	2.27	0.43	0.84	1.08	1.41	15.46	1.60	41.67	3.00	2.57	4.10	13.00
Current study	LIC-09_mod3	12.87	11.10	3.31	0.68	1.39	1.22	4.76	9.22	0.56	37.98	4.16	2.77	3.22	6.77
Current study	LIC-10	8.40	8.64	11.75	1.33	0.80	5.30	3.40	10.52	0.20	35.99	2.79	2.44	4.41	4.01

Table A.2. Glass IDs, sources, and compositions for glasses considered in the development of the ZrO_2-based constraint.

Source	Glass ID	Al_2O_3	B_2O_3	CaO	Cr_2O_3	Fe_2O_3	K_2O	Li_2O	Na_2O	SO_3	SiO_2	SnO_2	ZnO	ZrO_2	Others
PNNL-26630	New-OL-14844	3.50	6.15	12.24	0.31	0.00	1.50	5.00	15.51	0.10	34.00	0.00	5.00	6.50	10.19
PNNL-26630	New-OL-8788Mod	12.35	6.00	0.05	0.31	1.50	1.50	2.50	13.00	0.10	46.00	0.00	5.00	5.50	6.19
PNNL-26630	New-OL-8445	12.41	13.75	12.24	0.31	0.00	1.50	2.01	10.00	0.10	34.00	0.00	1.00	6.50	6.19
PNNL-28838, Rev. 2	LP2-IL-01	7.50	8.00	7.62	0.53	0.20	2.00	0.00	23.68	0.80	37.98	0.50	2.40	5.50	3.30
PNNL-28838, Rev. 2	LP2-IL-02	7.50	8.13	2.00	0.38	0.58	2.00	0.00	23.68	0.80	41.81	2.50	2.63	5.50	2.50
PNNL-28838, Rev. 2	LP2-IL-03	8.73	8.73	2.00	0.53	0.20	0.76	0.00	24.50	0.20	40.36	2.50	3.20	5.50	2.80
VSL-00R3501-1, Rev. 0	LAWBS1-G-36F	6.16	12.09	4.70	0.09	5.15	0.32	2.96	7.90	1.03	46.91	0.00	3.09	3.09	6.51
VSL-13R2940-1, Rev. 0	LORPM2R1	12.88	6.52	10.59	0.32	0.30	5.25	2.66	6.82	0.19	35.00	2.16	1.00	6.00	10.30
VSL-13R2940-1, Rev. 0	LORPM13	13.85	13.73	0.00	0.01	8.00	0.11	0.50	13.31	1.00	37.06	1.39	1.00	6.00	4.04

Table A.3. Glass IDs, sources, and compositions for glasses considered in the development of the both the SnO_2- and ZrO_2-based constraints. This table contains glasses with both crystals present in significant quantities (i.e., > 0.01 vol%).

Source	Glass ID	Al_2O_3	B_2O_3	CaO	Cl	Cr_2O_3	Fe_2O_3	K_2O	Li_2O	Na_2O	SO_3	SiO_2	SnO_2	ZnO	ZrO_2	Others
PNNL-26630	New-OL-62909Mod	12.35	8.90	12.24	0.31	0.00	0.00	2.50	13.00	0.10	33.50	4.41	1.00	5.50	6.19	12.35
VSL-07R1130-1, Rev. 0	ORPLA15	9.46	8.65	3.34	0.50	0.93	0.54	0.00	24.00	0.18	39.50	2.75	2.45	5.95	1.76	9.46
VSL-09R1510-2, Rev. 0	ORPLA21	6.91	8.64	3.28	0.50	0.29	0.56	0.00	25.00	0.19	41.72	2.71	2.71	5.88	1.62	6.91
VSL-09R1510-2, Rev. 0	ORPLA22	9.46	8.80	3.55	0.50	0.00	0.54	0.00	24.00	0.18	40.29	3.00	3.00	6.00	0.68	9.46
VSL-09R1510-2, Rev. 0	ORPLA23	9.46	8.80	3.55	0.50	0.00	0.54	0.00	24.00	0.18	40.29	5.00	3.00	4.00	0.68	9.46
VSL-09R1510-2, Rev. 0	ORPLA24	9.34	8.55	3.52	0.50	0.00	0.56	0.00	25.00	0.19	39.70	3.00	2.94	6.00	0.71	9.34
VSL-10R1790-1, Rev. 0	ORPLG13	6.54	8.28	2.62	0.57	0.28	5.47	0.00	20.00	0.39	39.76	2.76	3.31	5.52	4.51	6.54
VSL-10R1790-1, Rev. 0	ORPLG14	6.53	8.20	2.60	0.57	0.27	5.61	0.00	20.50	0.40	39.38	2.73	3.28	5.47	4.48	6.53
VSL-10R1790-1, Rev. 0	ORPLG15	6.51	8.12	2.57	0.57	0.27	5.75	0.00	21.00	0.41	39.00	2.71	3.25	5.41	4.44	6.51
VSL-10R1790-1, Rev. 0	ORPLG27	6.03	7.92	2.69	0.59	0.28	5.75	0.00	21.00	0.41	42.10	3.19	2.69	6.44	0.92	6.03
VSL-07R1130-1, Rev. 0	ORPLC1	9.50	6.06	3.00	0.50	1.00	0.58	0.00	25.00	0.55	38.32	2.00	3.00	4.50	6.02	9.50
VSL-01R3560-2, Rev. 0	LAWB44	6.07	11.92	4.63	0.09	13.20	0.31	0.00	7.79	4.44	46.23	0.00	4.02	3.05	0.14	6.07
VSL-01R3560-2, Rev. 0	LAWB51S	6.09	12.54	6.74	0.11	5.34	0.23	4.73	5.00	1.50	48.88	0.00	3.18	3.18	3.18	6.09
VSL-01R3560-2, Rev. 0	LAWB34	6.16	12.09	6.05	0.09	5.15	0.32	2.96	7.90	1.03	46.91	0.00	3.09	3.09	5.17	6.16

Appendix B – Images of As-Melted LIC Glasses

This appendix shows images of the 10 low-activity waste isothermal crystallization (LIC) glasses studied during this effort after their final melts.

Figure B.1. LIC-01 final melt.

Figure B.2. LIC-02-MOD2 final melt

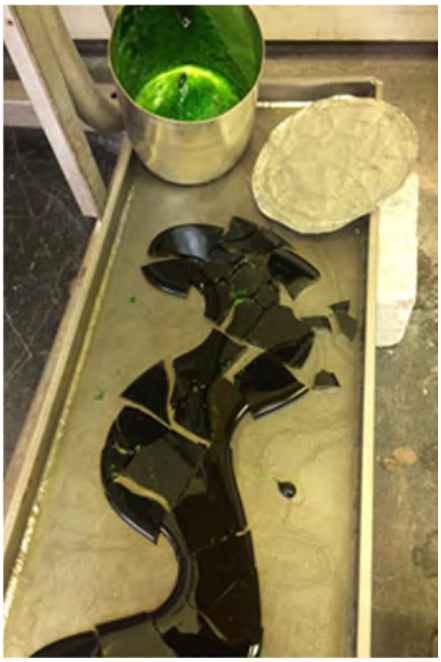

Figure B.3. LIC-03 final melt

Figure B.4. LIC-04-MOD1 final melt.

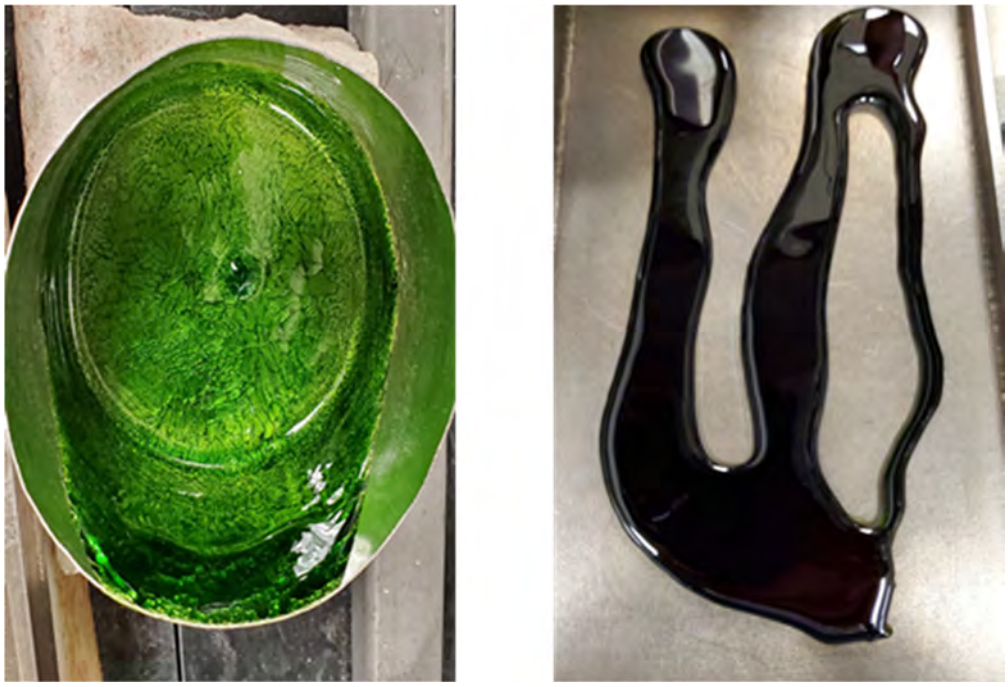

Figure B.5. LIC-05 final melt.

Figure B.6. LIC-06 final melt.

Figure B.7. LIC-07 final melt.

Figure B.8. LIC-08 final melt.

Figure B.9. LIC-09-MOD3 final melt.

Figure B.10. LIC-10 final melt.

Appendix C – Images of LIC Glasses after Heat Treatment

This appendix contains images of the glasses in this study after isothermal heat treatment at various temperatures for the indicated times.

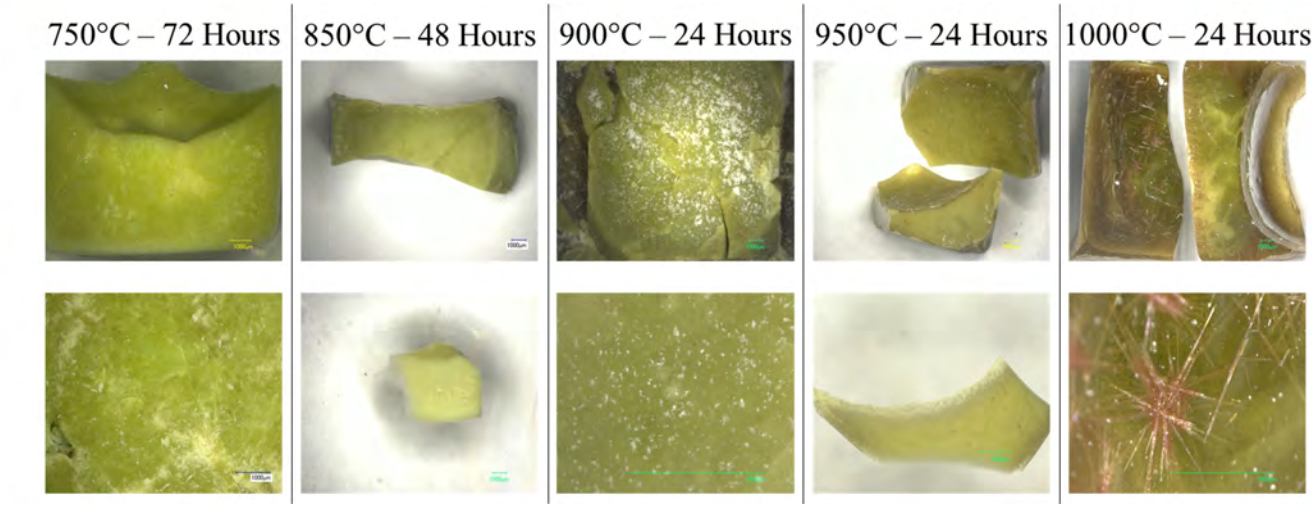

Figure C.1. Optical images of heat-treated of LIC-01 glasses.

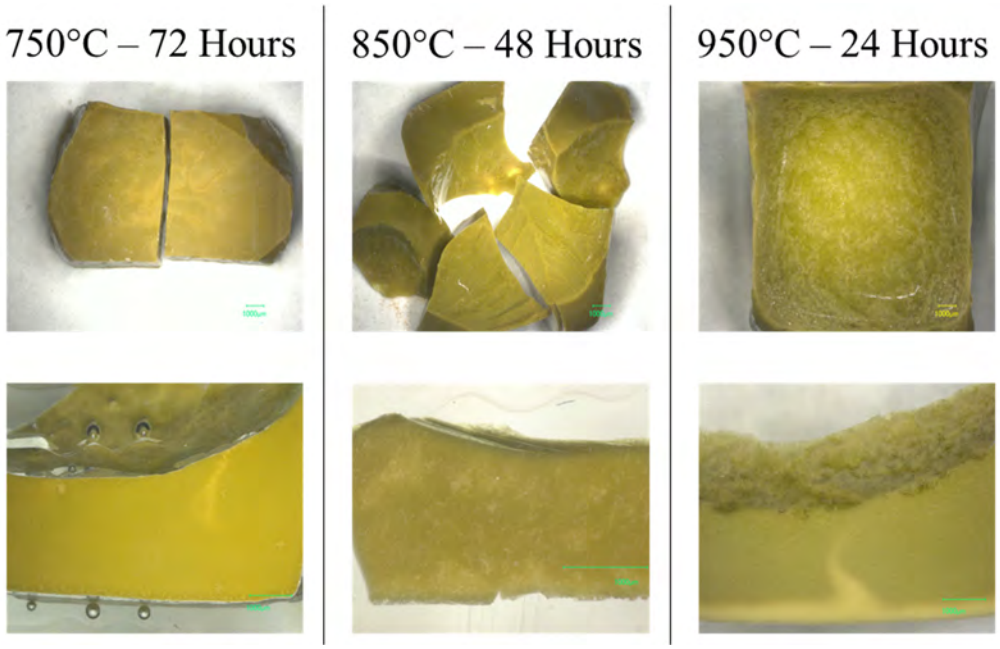

Figure C.2. Optical images of heat-treated LIC-02 second modification glasses

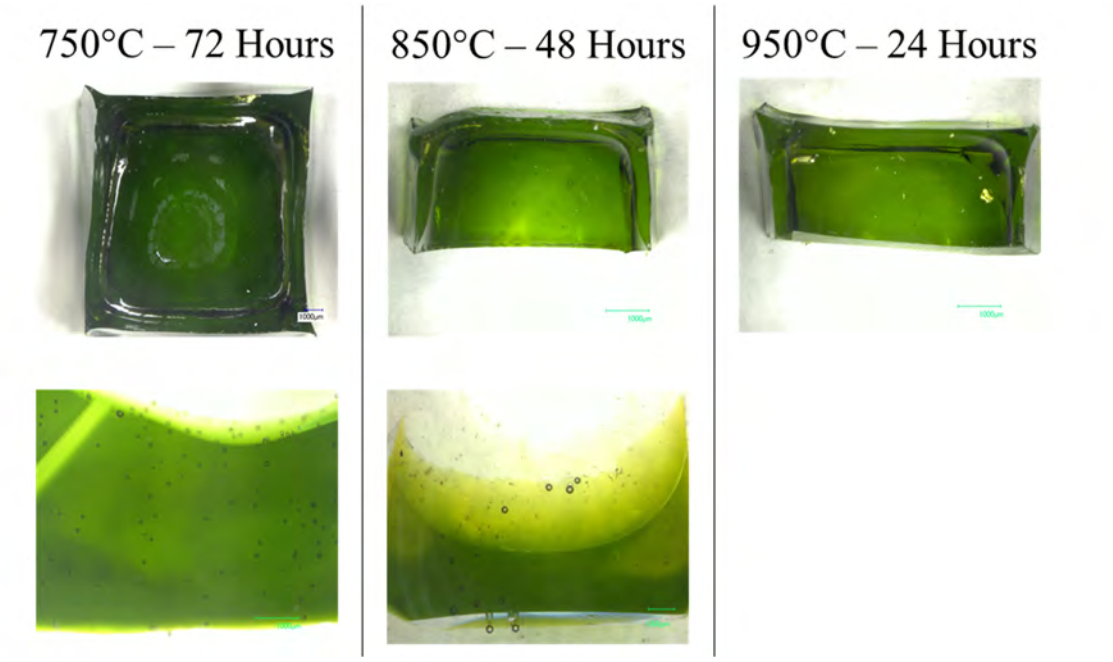

Figure C.3. Optical images of heat-treated LIC-03 glasses.

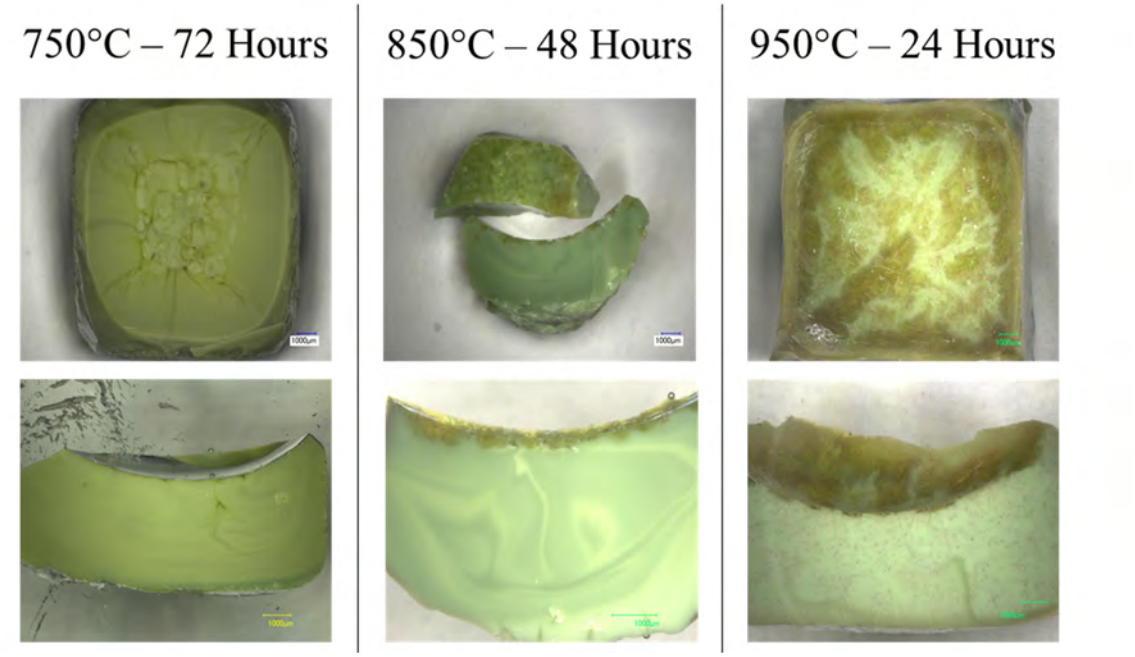

Figure C.4. Optical images of heat-treated LIC-04 first modification glasses.

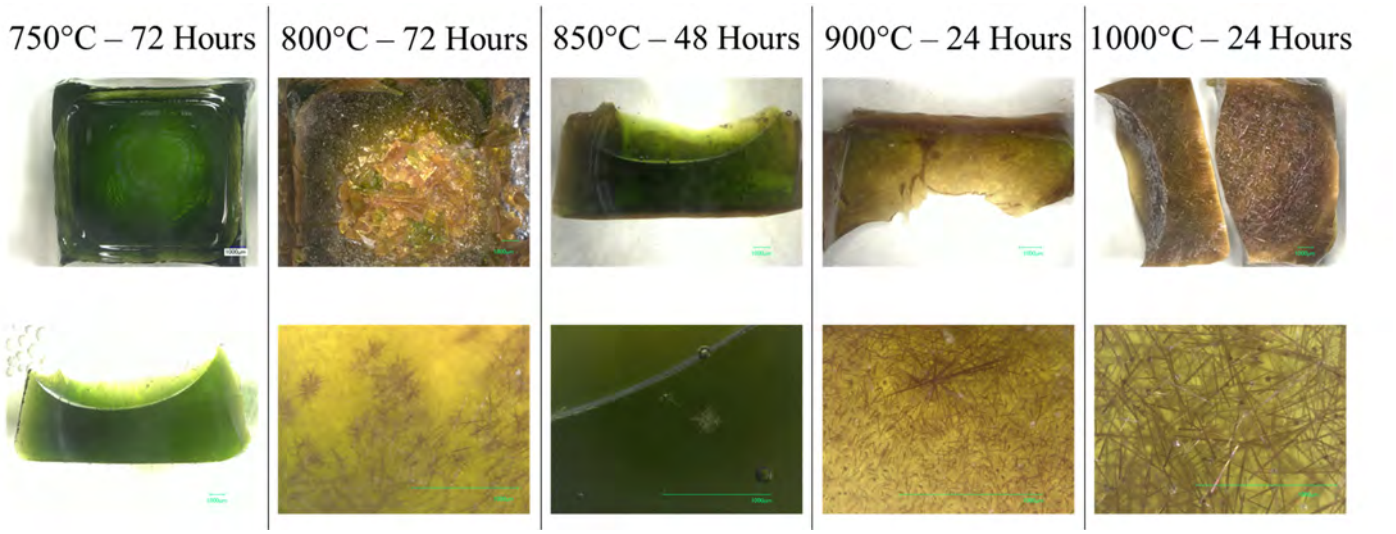

Figure C.5. Optical images of heat-treated LIC-05 glasses.

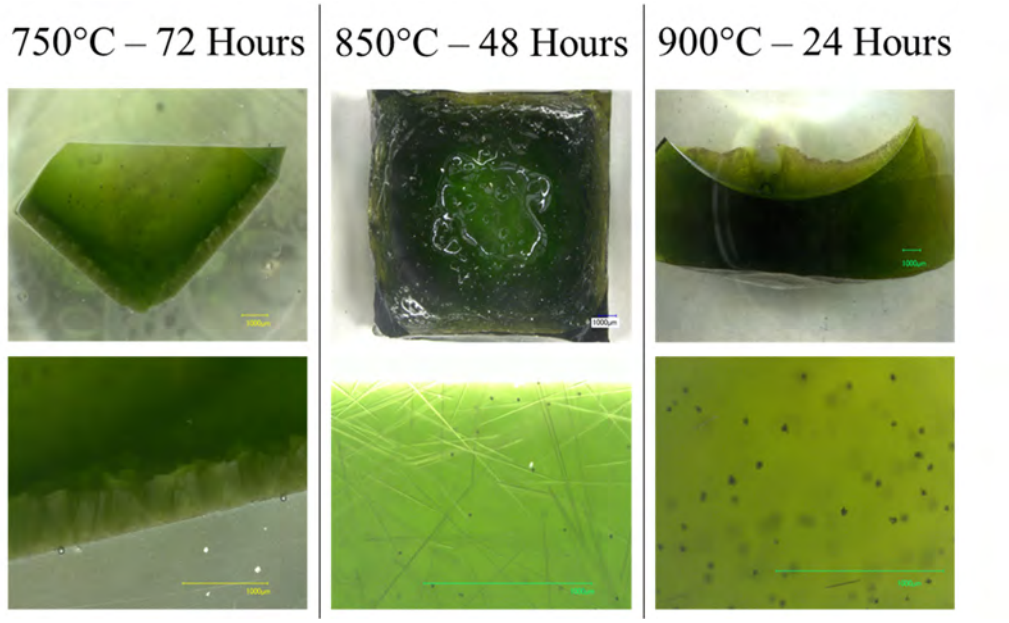

Figure C.6. Optical images of heat-treated LIC-06 glasses.

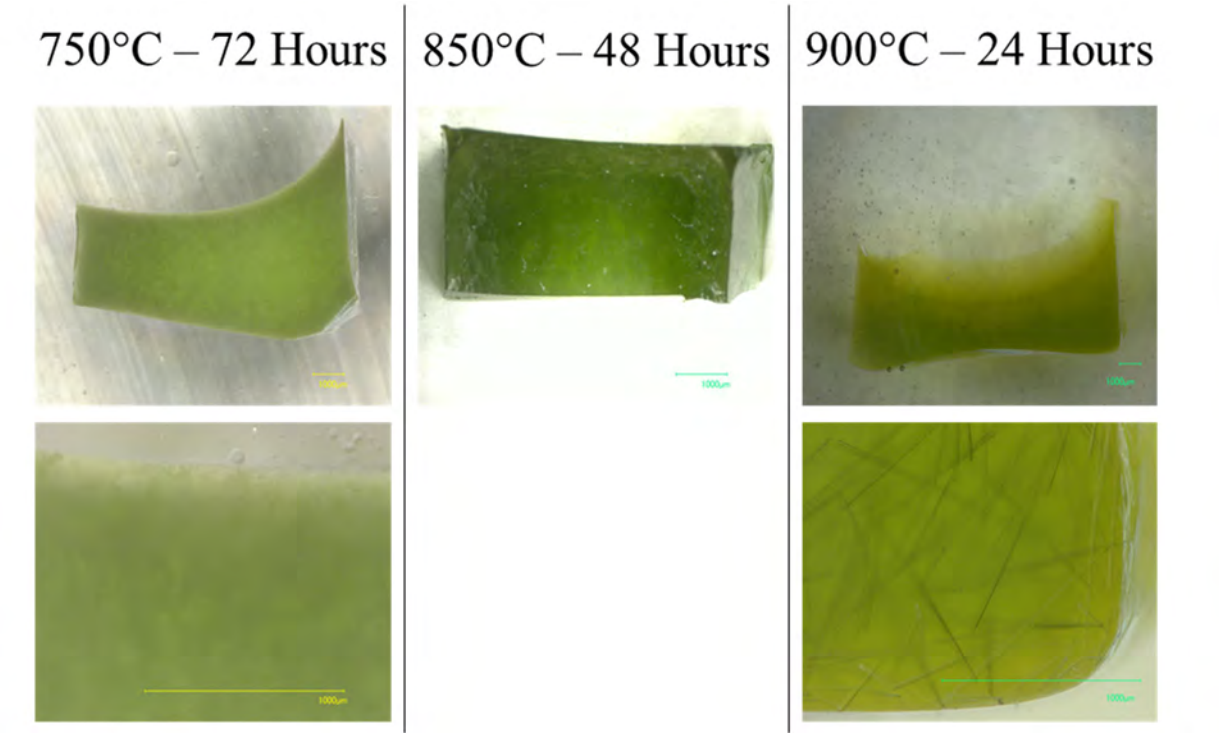

Figure C.7. Optical images of heat-treated LIC-07 glasses.

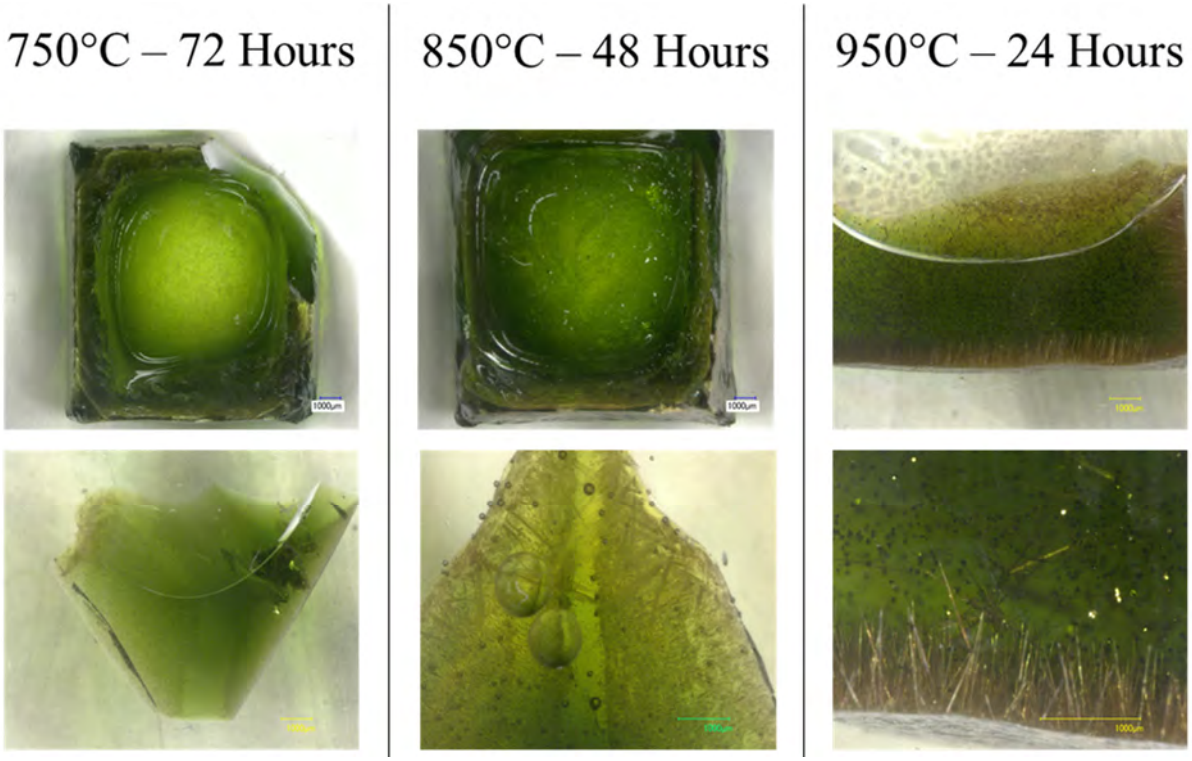

Figure C.8. Optical images of heat-treated LIC-08 glasses.

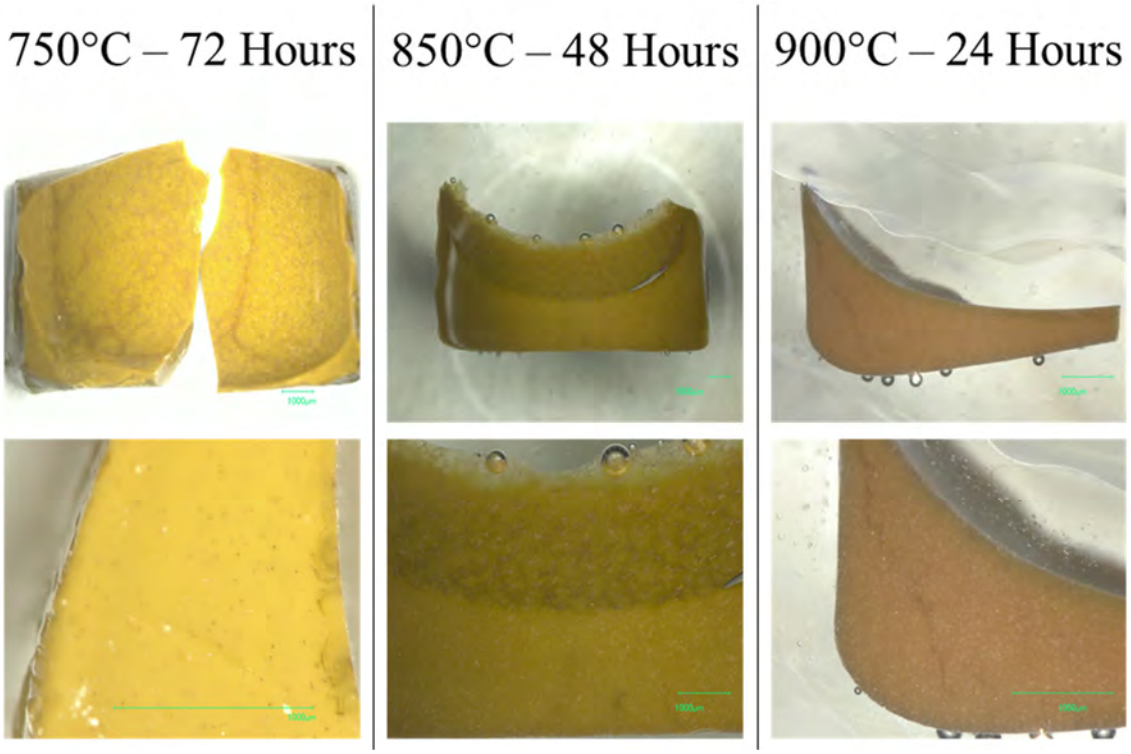

Figure C.9. Optical images of heat-treated LIC-09 third modification glasses.

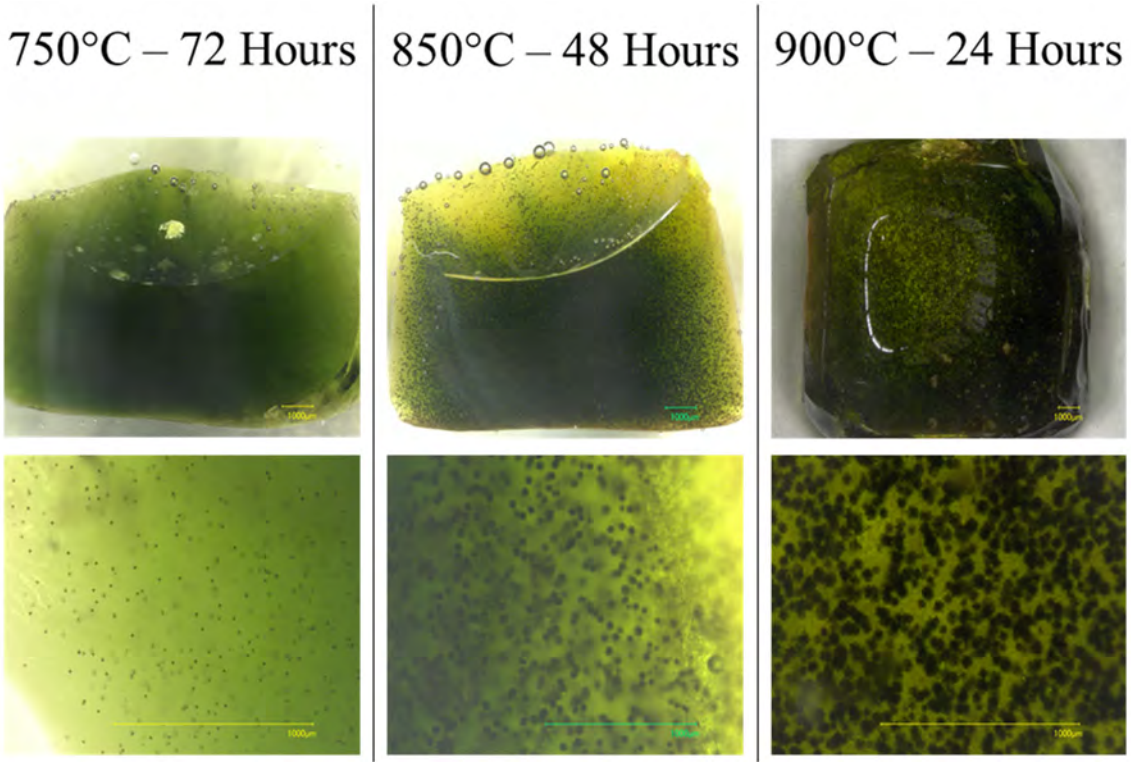

Figure C.10. Optical images of heat-treated LIC-10 glasses.

Appendix D – X-Ray Diffraction Data for LIC Glasses

This appendix contains X-ray diffraction (XRD) data for the low-activity waste isothermal crystallization (LIC) glasses after quench and upon various isothermal heat treatments. The diffractograms as well as the corresponding tables with phase identification and quantification are shown for each of the 10 glasses. CeO_2 was used as the internal standard for all samples.

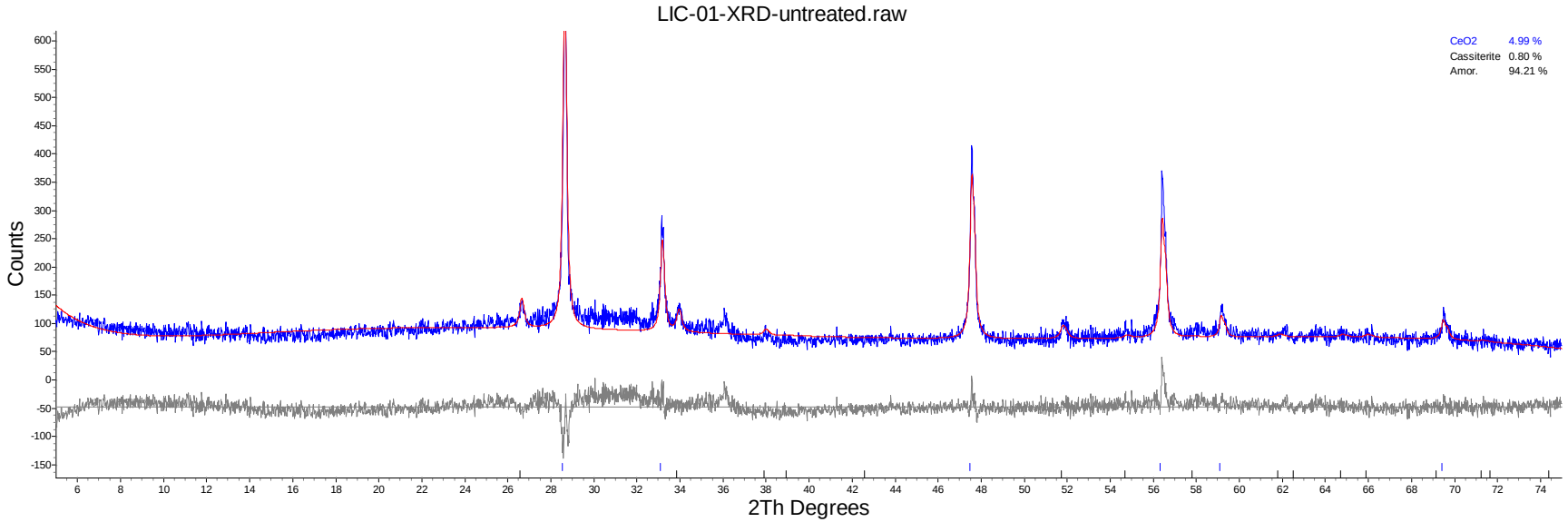

Figure D.1. XRD data for LIC-01 final melt.

Table D.1. XRD data for LIC-01 final melt.

Phase Name	Wt% of Spike	Wt% in Spiked Sample	Wt% in Original Sample
CeO_2	4.99	4.99	0
Cassiterite	0	0.80	0.84

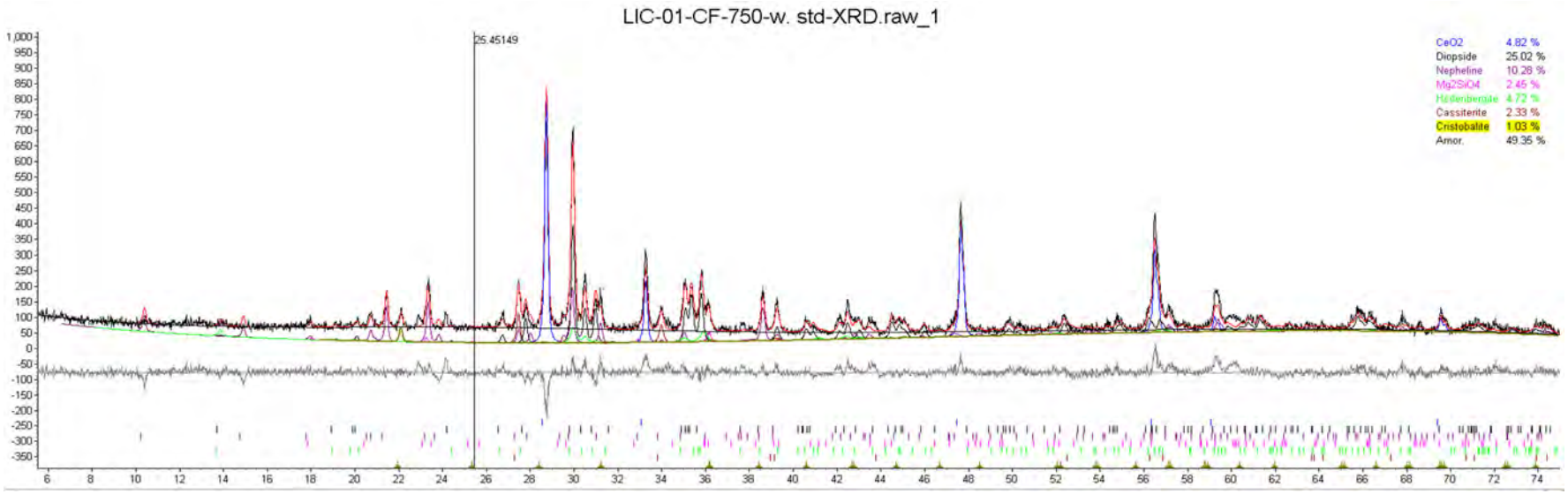

Figure D.2. XRD data for LIC-01-CF-750.

Table D.2. XRD data for LIC-01-CF-750

Phase Name	Wt% of Spike	Wt% in Spiked Sample	Wt% in Original Sample
CeO_2	4.82	4.82	0.00
Diopside	0	25.02	26.29
Nepheline	0	10.28	10.80
Mg_2SiO_4 (Forsterite)	0	2.45	2.57
Hedenbergite	0	4.73	4.96
Cassiterite	0	2.33	2.44
Cristobalite	0	1.03	1.08

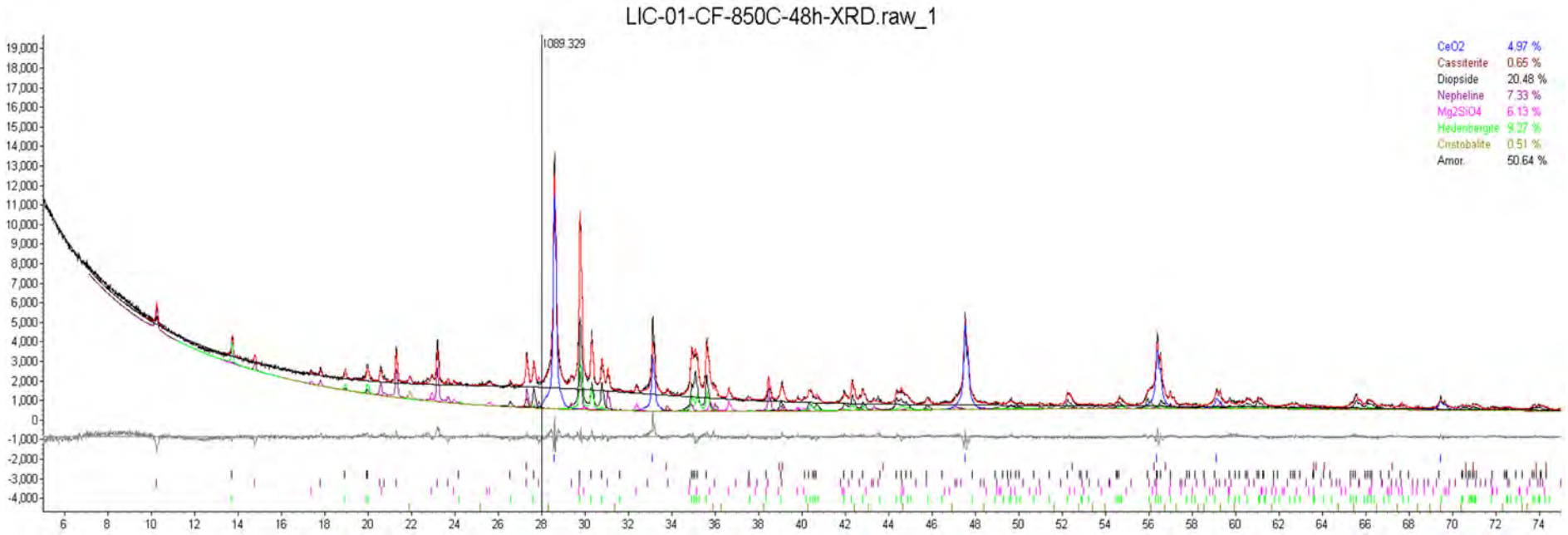

Figure D.3. XRD data for LIC-01-CF-850C-48hr.

Table D.3. XRD data for LIC-01-CF-850C-48hr.

Phase Name	Wt% of Spike	Wt% in Spiked Sample	Wt% in Original Sample
CeO_2	4.97	4.97	0.00
Diopside	0	20.48	21.55
Nepheline	0	7.33	7.72
Mg_2SiO_4	0	6.13	6.45
Hedenbergite	0	9.27	9.76
Cassiterite	0	0.65	0.69
Cristobalite	0	0.52	0.54

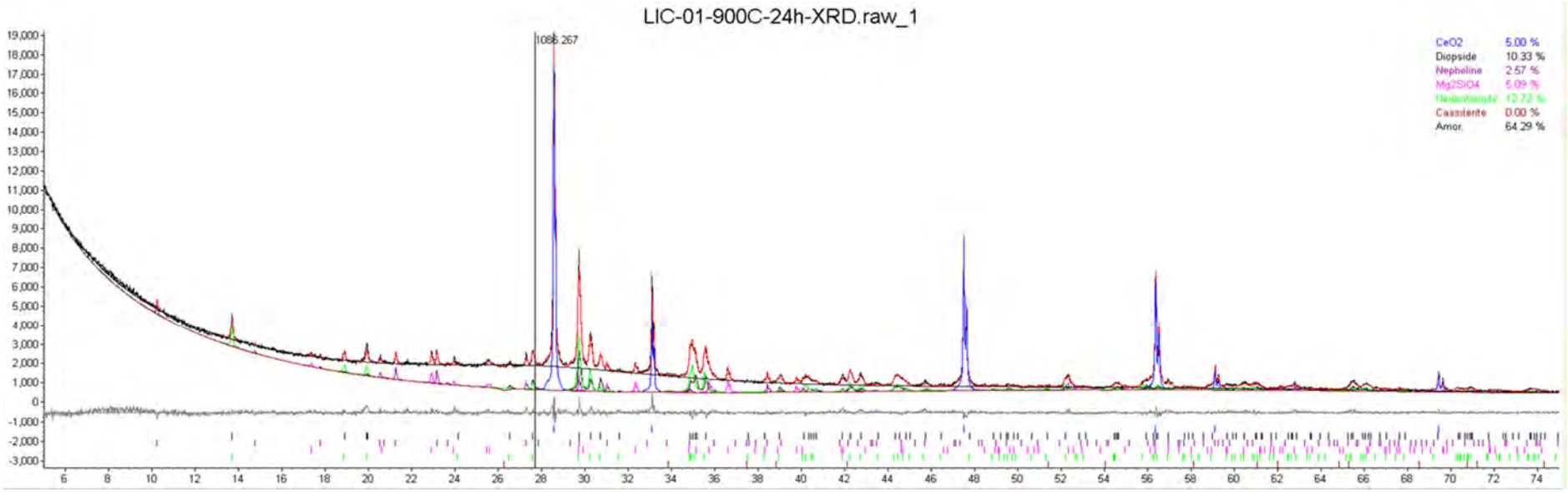

Figure D.4. XRD data for LIC-01-900C-24hr.

Table D.4. XRD data for LIC-01-900C-24hr.

Phase Name	Wt% of Spike	Wt% in Spiked Sample	Wt% in Original Sample
CeO_2	5.00	5.00	0
Diopside	0	10.33	10.87
Nepheline	0	2.57	2.71
Mg_2SiO_4	0	5.09	5.36
Hedenbergite	0	12.72	13.39
Cassiterite	0	0.01	0.01

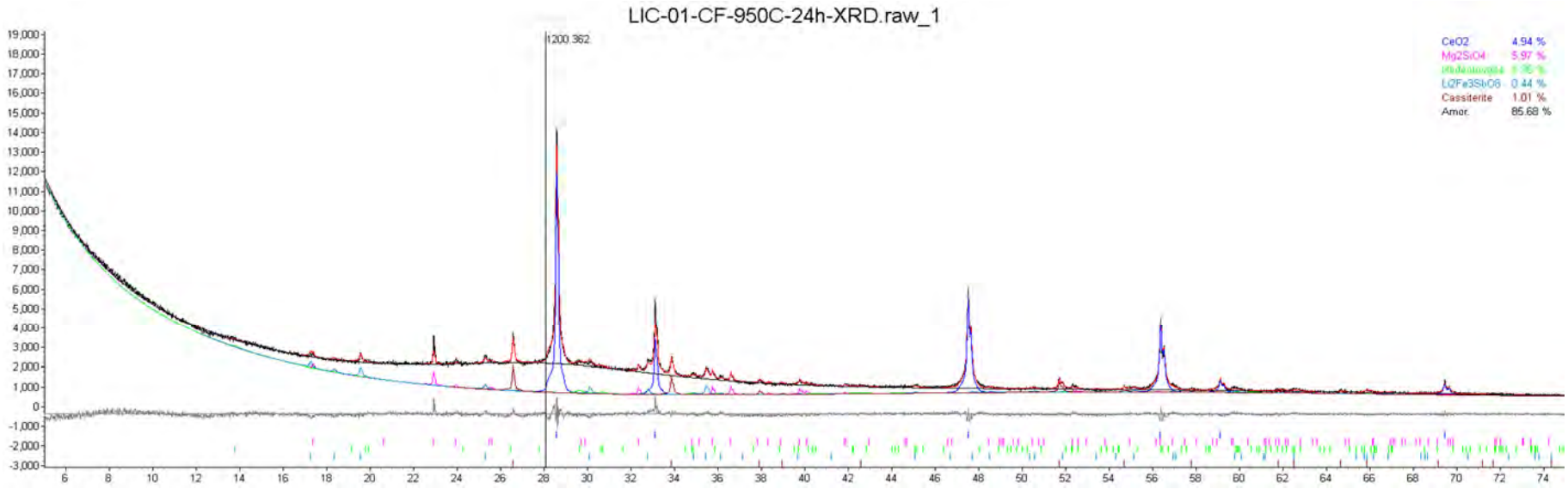

Figure D.5. XRD data for LIC-01-CF-950C-24hr.

Table D.5. XRD data for LIC-01-CF-950C-24hr.

Phase Name	Wt% of Spiked	Wt% in Spiked Sample	Wt% in Original Sample
CeO_2	4.94	4.94	0.00
Mg_2SiO_4	0	5.97	6.28
Hedenbergite	0	1.96	2.06
$Li_2Fe_3SbO_8$	0	0.44	0.46
Cassiterite	0	1.01	1.07

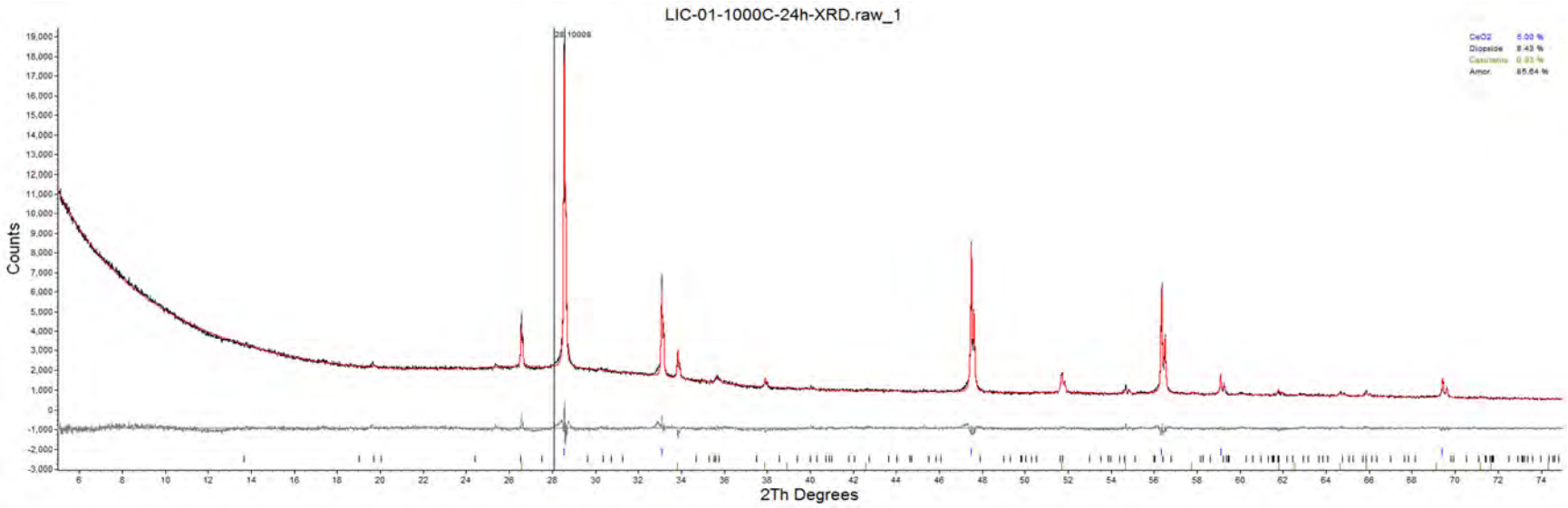

Figure D.6. XRD data for LIC-01-1000C-24hr.

Table D.6. XRD data for LIC-01-1000C-24hr.

Phase Name	Wt% of Spike	Wt% in Spiked Sample	Wt% in Original Sample
CeO_2	5.00	5.00	0
$Li_2Fe_3SbO_8$	0	0.35	0.36
Cassiterite	0	1.44	1.52

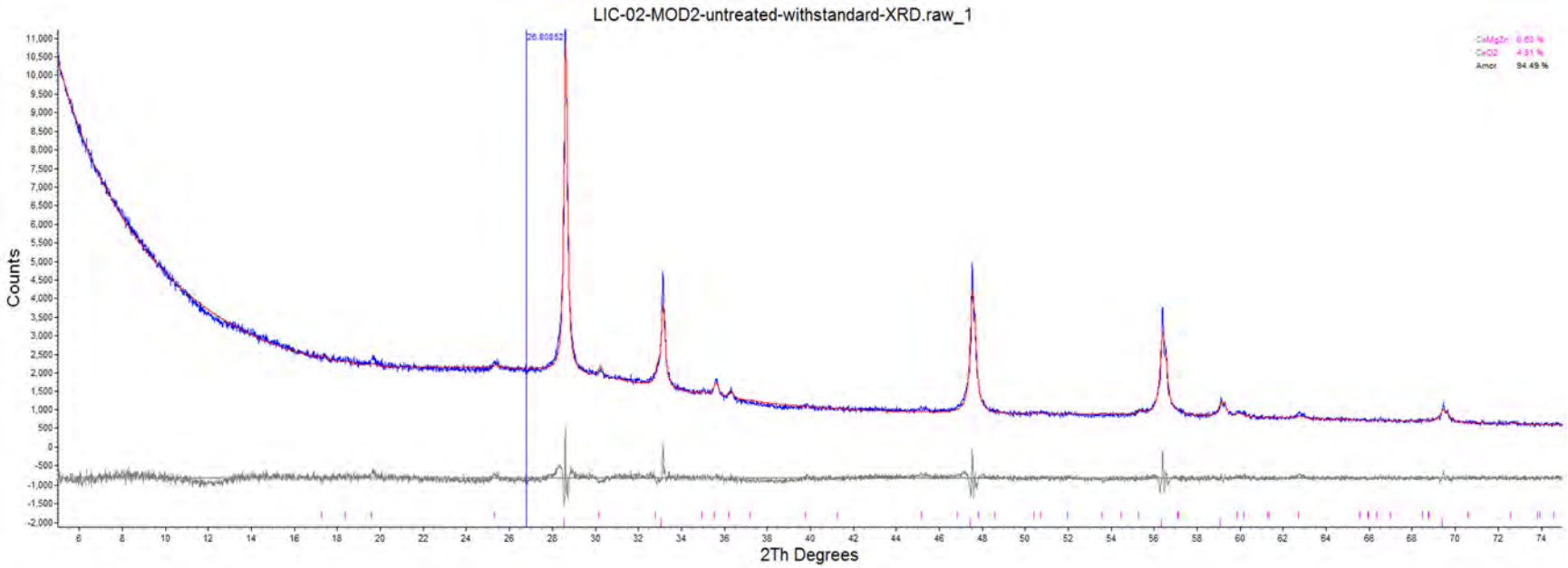

Figure D.7. XRD data for LIC-02-MOD2 final melt.

Table D.7. XRD data for LIC-02-MOD2 final melt.

Phase Name	Wt% of Spike	Wt% in Spiked Sample	Wt% in Original Sample
CaMgZn	0	0.60	0.64
CeO_2	4.91	4.91	0

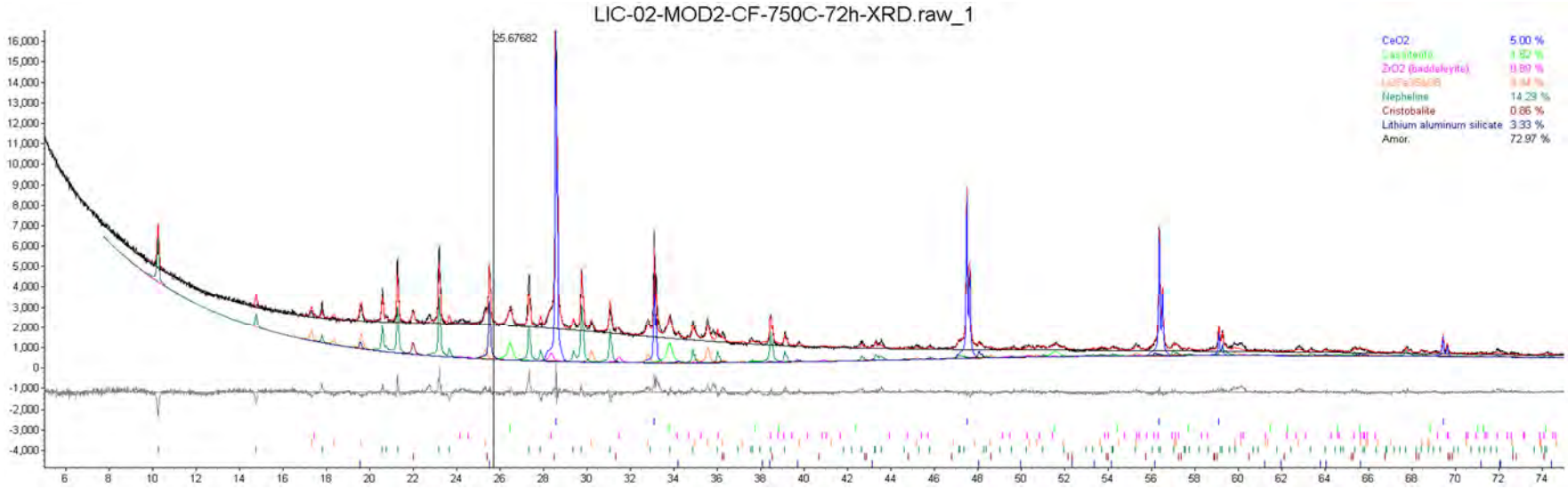

Figure D.8. XRD data for LIC-02-MOD2-750C-72hr.

Table D.8. XRD data for LIC-02-MOD2-750C-72hr.

Phase Name	Wt% of Spike	Wt% in Spiked Sample	Wt% in Original Sample
CeO_2	5.00	5.00	0.00
Cassiterite	0	1.82	1.91
ZrO_2 (baddeleyite)	0	0.89	0.94
$Li_2Fe_3SbO_8$	0	0.84	0.89
Nepheline	0	14.29	15.04
Cristobalite	0	0.86	0.91
Lithium aluminum silicate	0	3.33	3.51

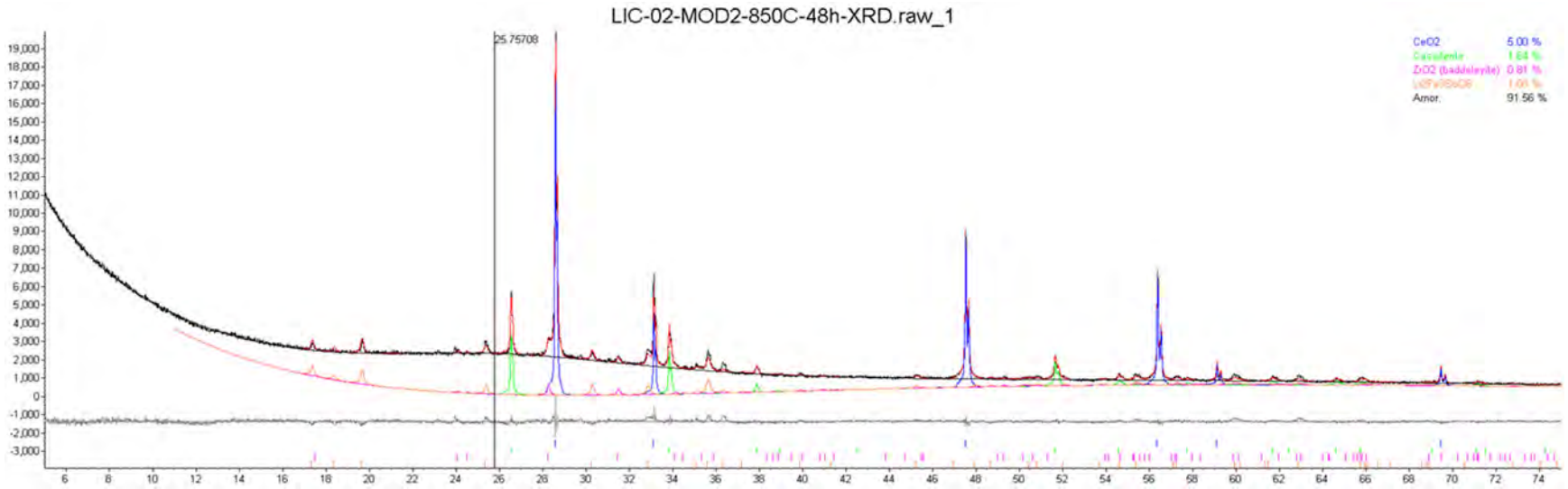

Figure D.9. XRD data for LIC-02-MOD2-850C-48hr.

Table D.9. XRD data for LIC-02-MOD2-850C-48hr.

Phase Name	Wt% of Spike	Wt% in Spiked Sample	Wt% in Original Sample
CeO_2	5.00	5.00	0.00
Cassiterite	0.00	1.64	1.72
ZrO_2 (baddeleyite)	0.00	0.81	0.85
$Li_2Fe_3SbO_8$	0.00	1.00	1.05

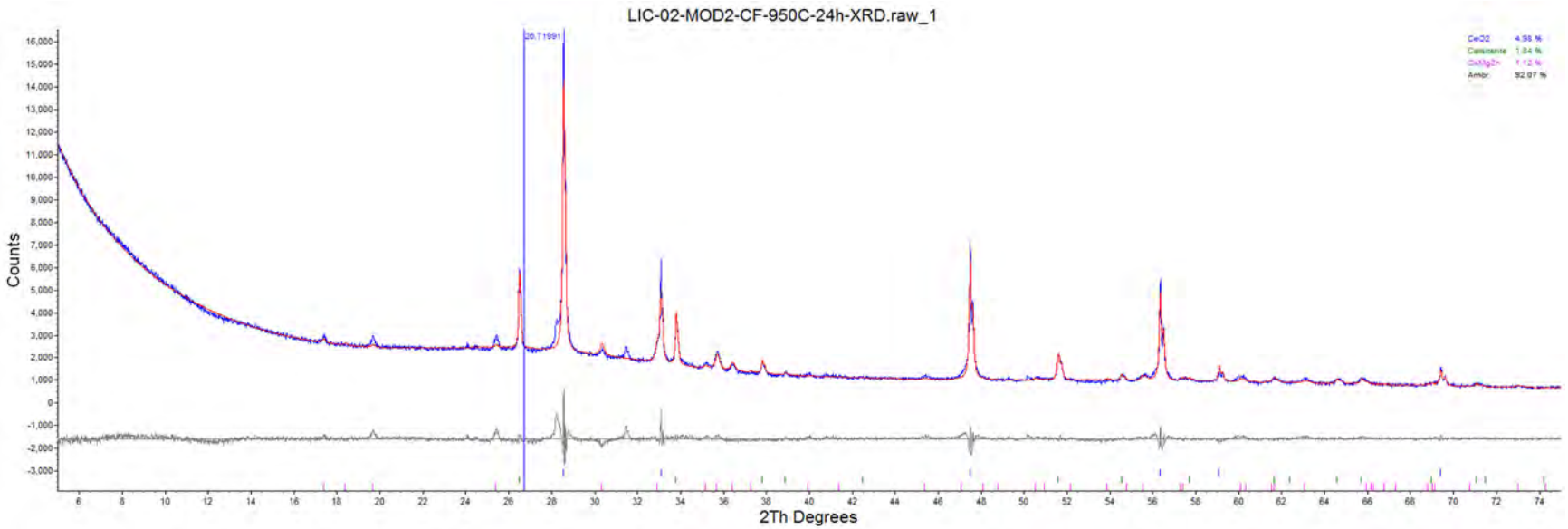

Figure D.10. XRD data for LIC-02-MOD2 -950C-24hr.

Table D.10. XRD data for LIC-02-MOD2 -950C-24hr.

Phase Name	Wt% of Spike	Wt% in Spiked Sample	Wt% in Original Sample
CeO_2	4.98	4.98	0.00
Cassiterite	0.00	1.76	1.85
ZrO_2 (baddeleyite)	0.00	1.48	1.56
$Li_2Fe_3SbO_8$	0.00	0.84	0.89

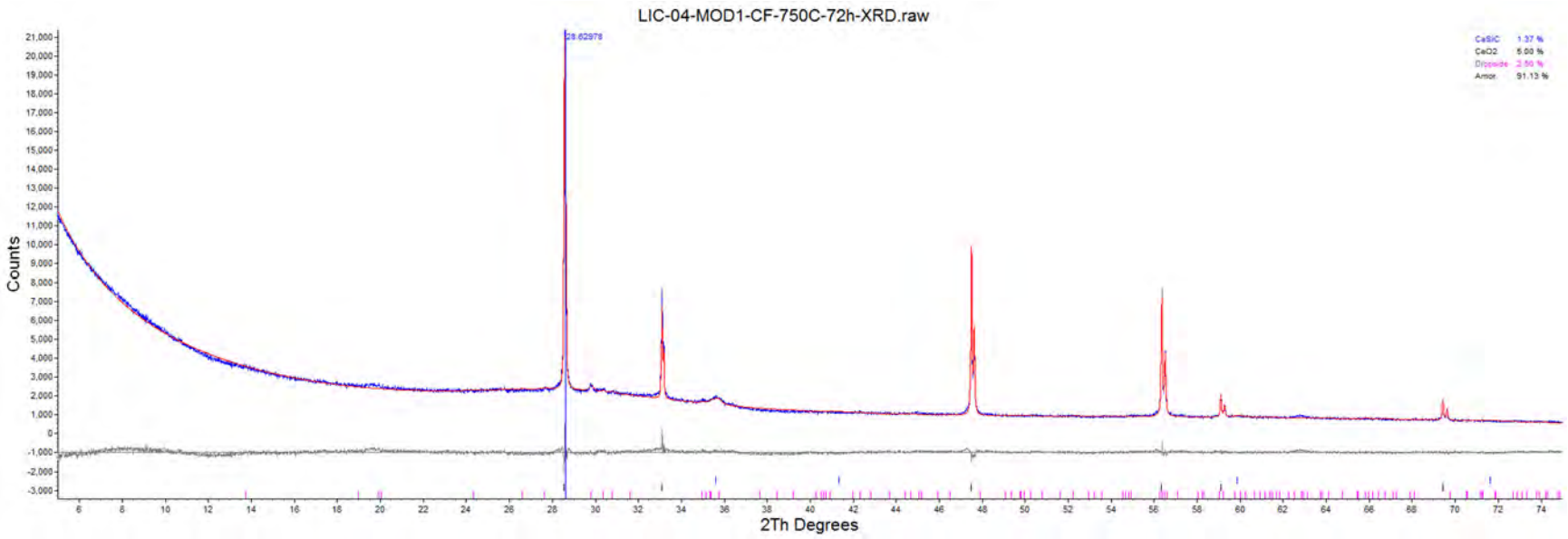

Figure D.11. XRD data for LIC-04-MOD1-750C-72h.

Table D.11. XRD data for LIC-04-MOD1-750C-72h.

Phase Name	Wt% of Spike	Wt% in Spiked Sample	Wt% in Original Sample
CeO_2	5.00	5.00	0.00
$Li_2Fe_3SbO_8$	0.00	0.65	0.69
Diopside	0.00	2.26	2.38

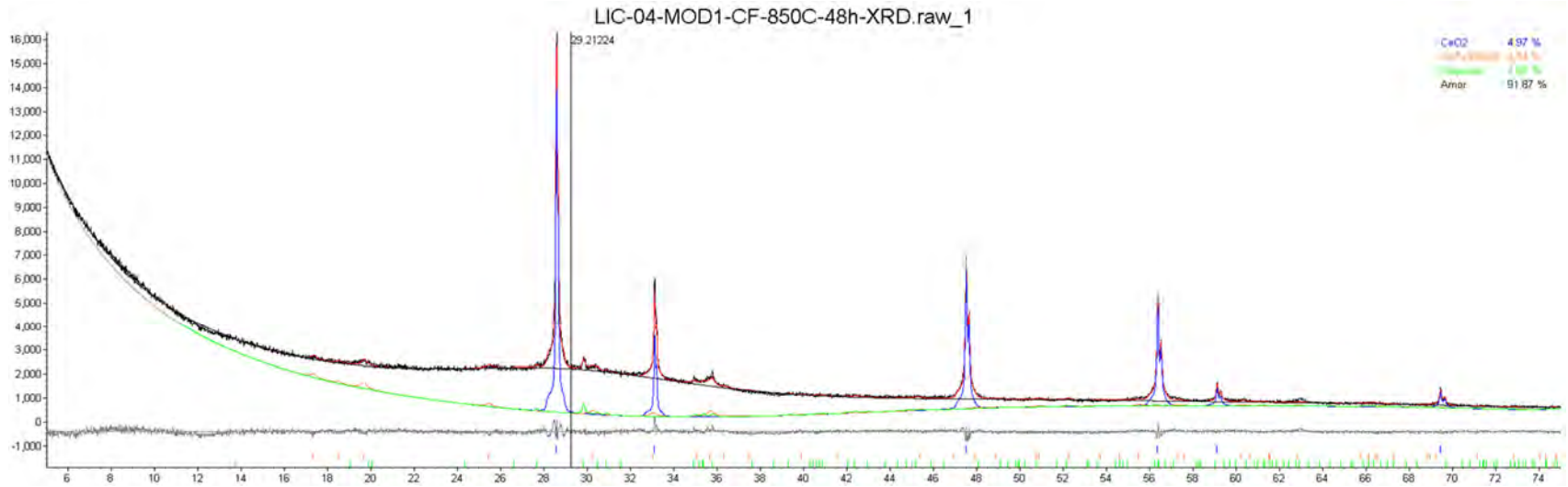

Figure D.12. XRD data for LIC-04-MOD1-850C-48h.

Table D.12. XRD data for LIC-04-MOD1-850C-48h.

Phase Name	Wt% of Spike	Wt% in Spiked Sample	Wt% in Original Sample
CeO_2	4.97	4.97	0.00
$Li_2Fe_3SbO_8$	0.00	0.54	0.57
Diopside	0.00	2.62	2.75

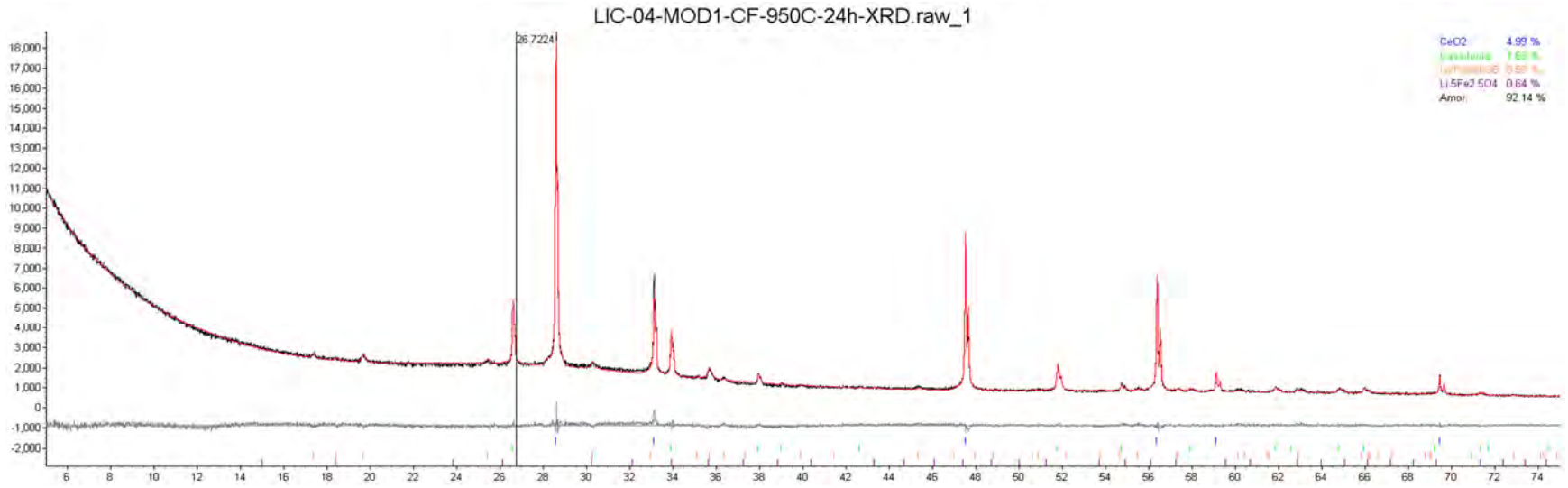

Figure D.13. XRD data for LIC-04-MOD1-950C-48h.

Table D.13. XRD data for LIC-04-MOD1-950C-48h.

Phase Name	Wt% of Spike	Wt% in Spiked Sample	Wt% in Original Sample
CeO_2	4.99	4.99	0.00
Cassiterite	0.00	1.63	1.72
$Li_2Fe_3SbO_8$	0.00	0.60	0.63
$Li_{0.5}Fe_{2.5}O_4$	0.00	0.64	0.67

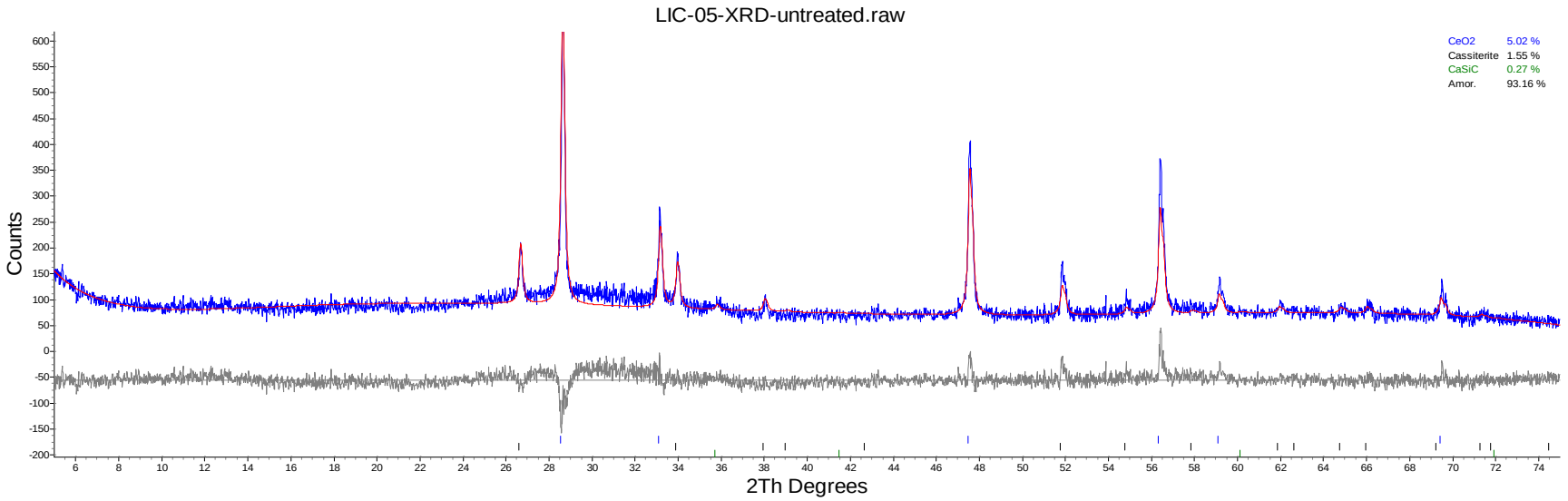

Figure D.14. XRD data for LIC-05 final melt.

Table D.14. XRD data for LIC-05 final melt.

Phase Name	Wt% of Spike	Wt% in Spiked Sample	Wt% in Original Sample
CeO_2	5.02	5.02	0
Cassiterite	0	1.55	1.63
CaSiC	0	0.27	0.29

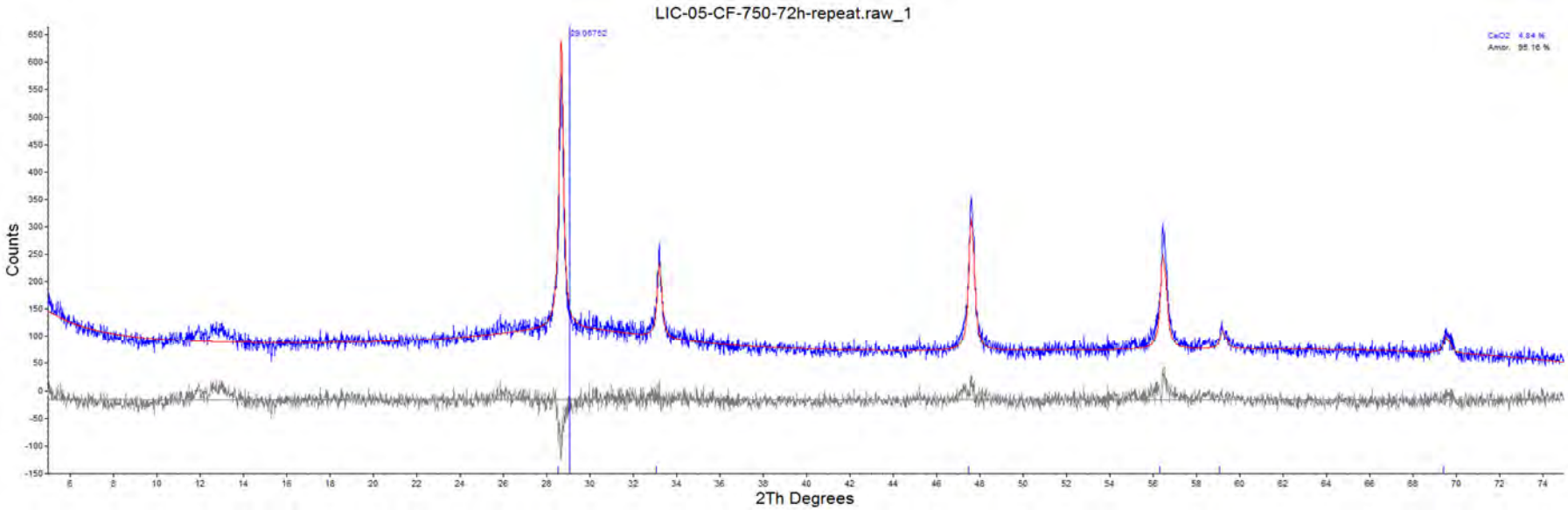

Figure D.15. XRD data for LIC-05-CF-750-72h.

Table D.15. XRD data for LIC-05-CF-750-72h.

Phase Name	Wt% of Spike	Wt% in Spiked Sample	Wt% in Original Sample
CeO_2	4.84	4.84	0

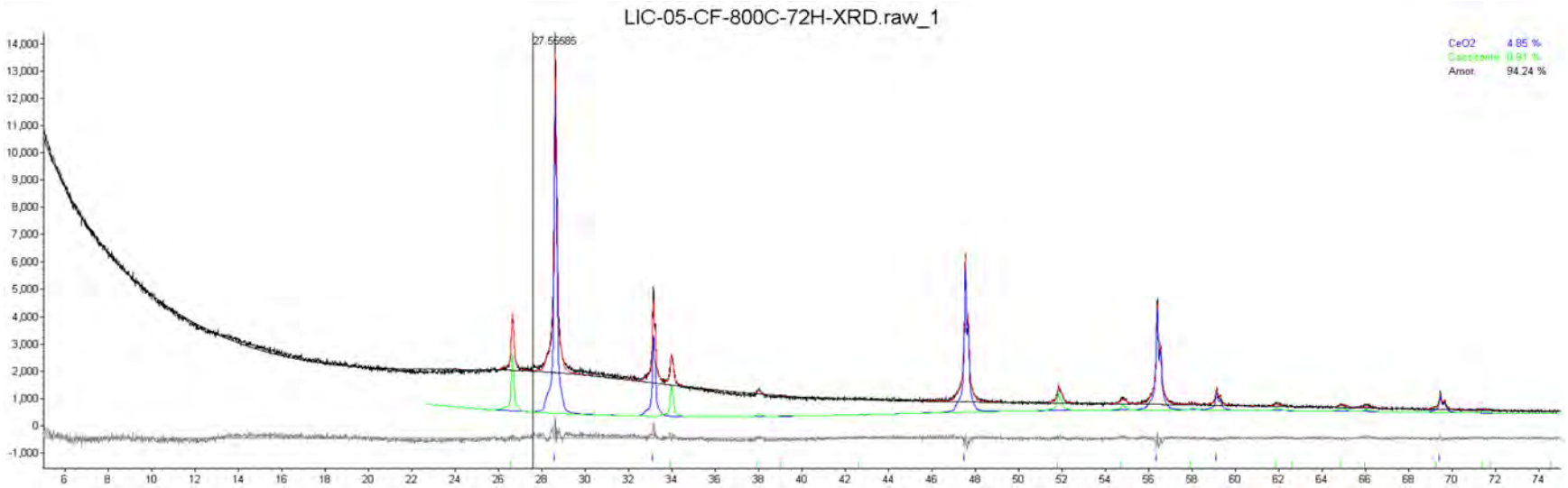

Figure D.16. XRD data for LIC-05-CF-800C-72h.

Table D.16. XRD data for LIC-05-CF-800C-72h.

Phase Name	Wt% of Spike	Wt% in Spiked Sample	Wt% in Original Sample
CeO_2	4.85	4.85	0.00
Cassiterite	0.00	0.91	0.95

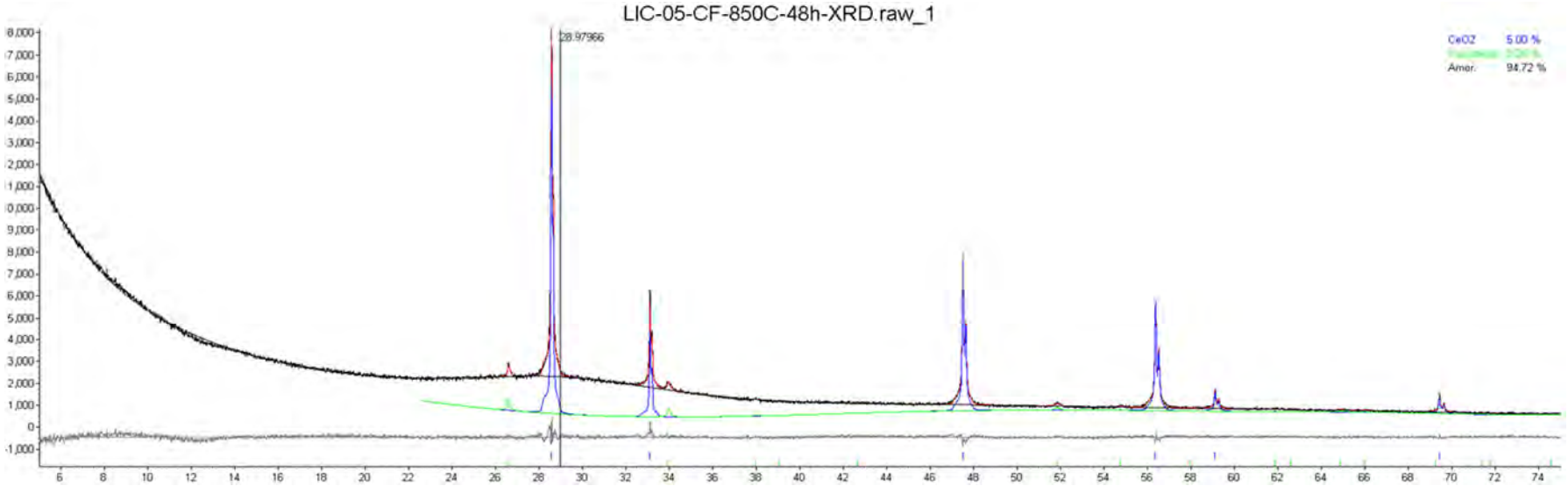

Figure D.17. XRD data for LIC-05-CF-850C-48h.

Table D.17. XRD data for LIC-05-CF-850C-48h.

Phase Name	Wt% of Spike	Wt% in Spiked Sample	Wt% in Original Sample
CeO_2	5.00	5.00	0.00
Cassiterite	0.00	0.28	0.30

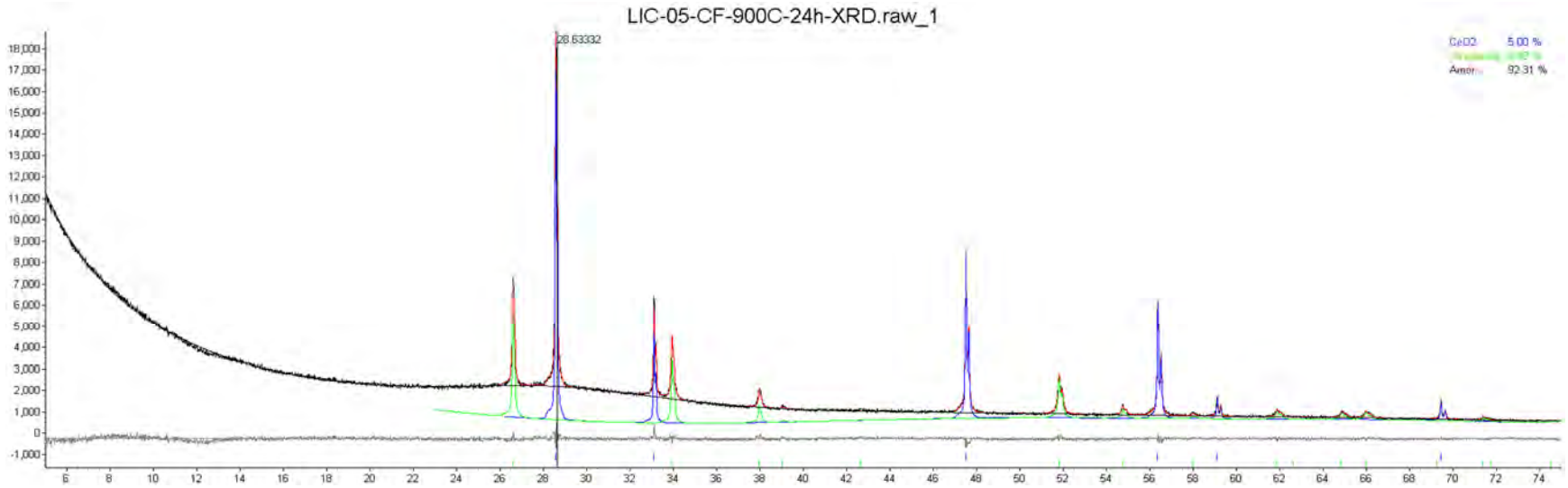

Figure D.18. XRD data for LIC-05-900C-24h.

Table D.18. XRD data for LIC-05-900C-24h.

Phase Name	Wt% of Spike	Wt% in Spiked Sample	Wt% in Original Sample
CeO_2	5.00	5.00	0.00
Cassiterite	0.00	2.69	2.83

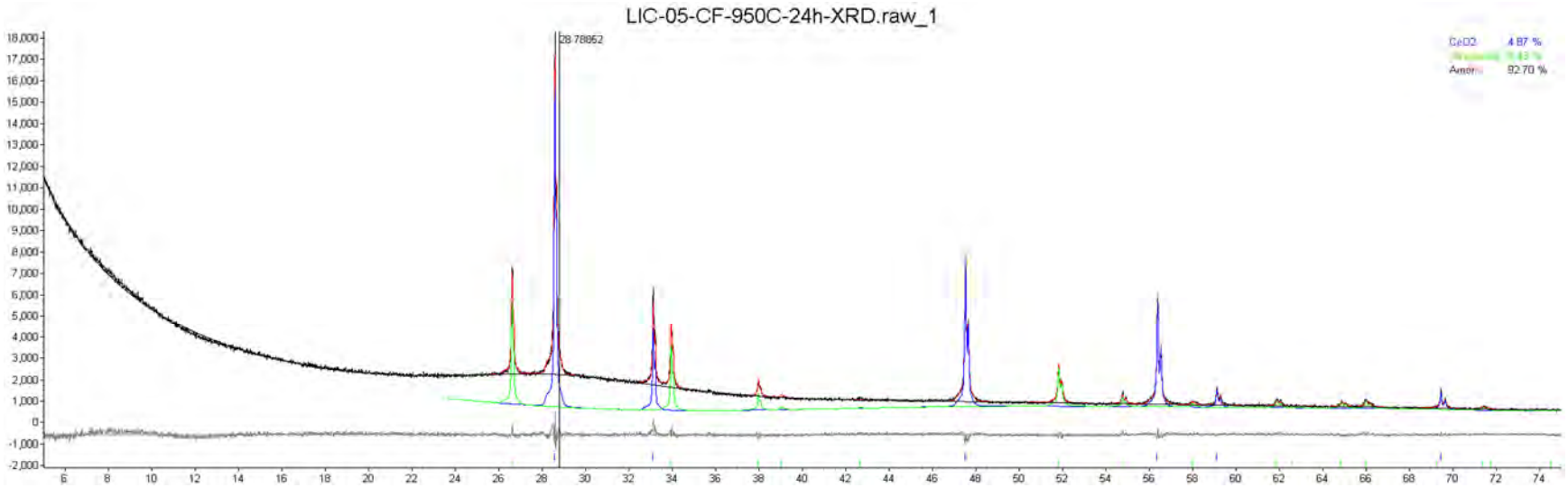

Figure D.19. XRD data for LIC-05-CF-950C-24h.

Table D.19. XRD data for LIC-05-CF-950C-24h.

Phase Name	Wt% of Spike	Wt% in Spiked Sample	Wt% in Original Sample
CeO_2	4.87	4.87	0.00
Cassiterite	0.00	2.43	2.55

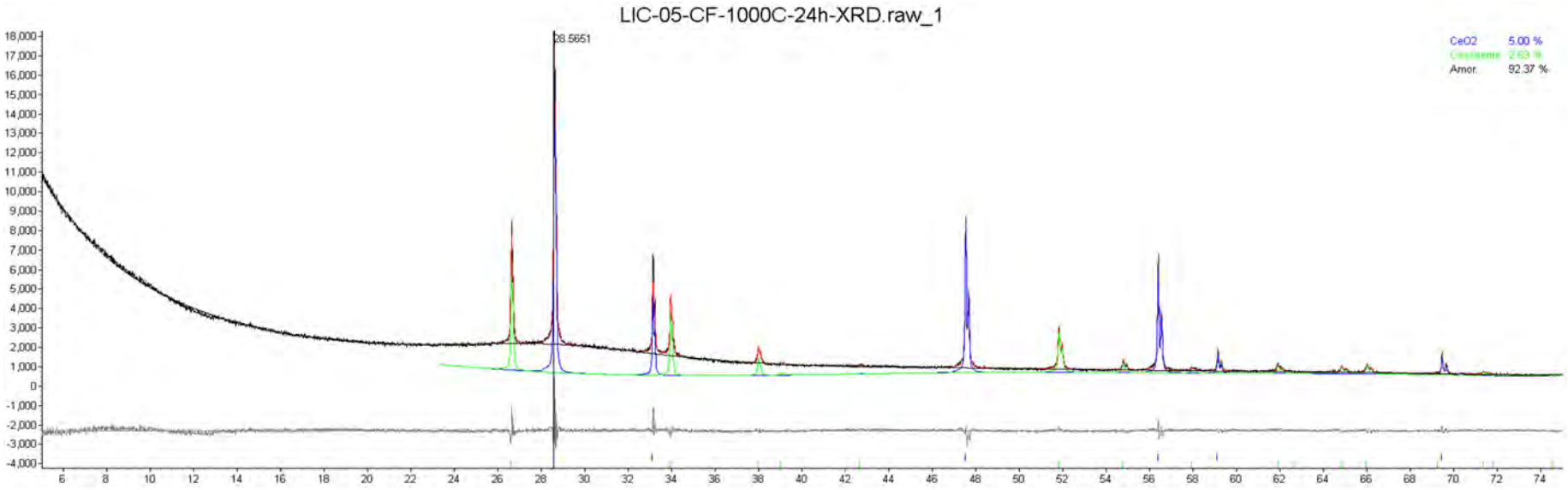

Figure D.20. XRD data for LIC-05-1000C-24h.

Table D.20. XRD data for LIC-05-1000C-24h.

Phase Name	Wt% of Spike	Wt% in Spiked Sample	Wt% in Original Sample
CeO_2	5.00	5.00	0.00
Cassiterite	0.00	2.63	2.77

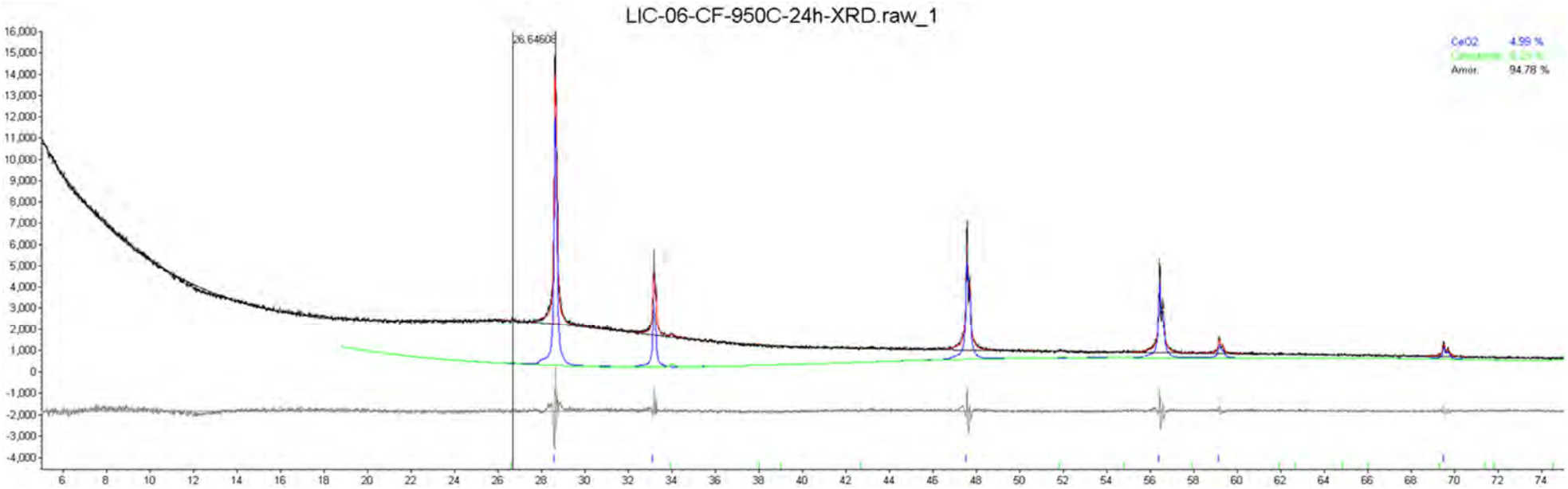

Figure D.21. XRD data for LIC-06-CF-950C-24h.

Table D.21. XRD data for LIC-06-CF-950C-24h.

Phase Name	Wt% of Spike	Wt% in Spiked Sample	Wt% in Original Sample
CeO_2	4.99	4.99	0.00
Cassiterite	0.00	0.23	0.24

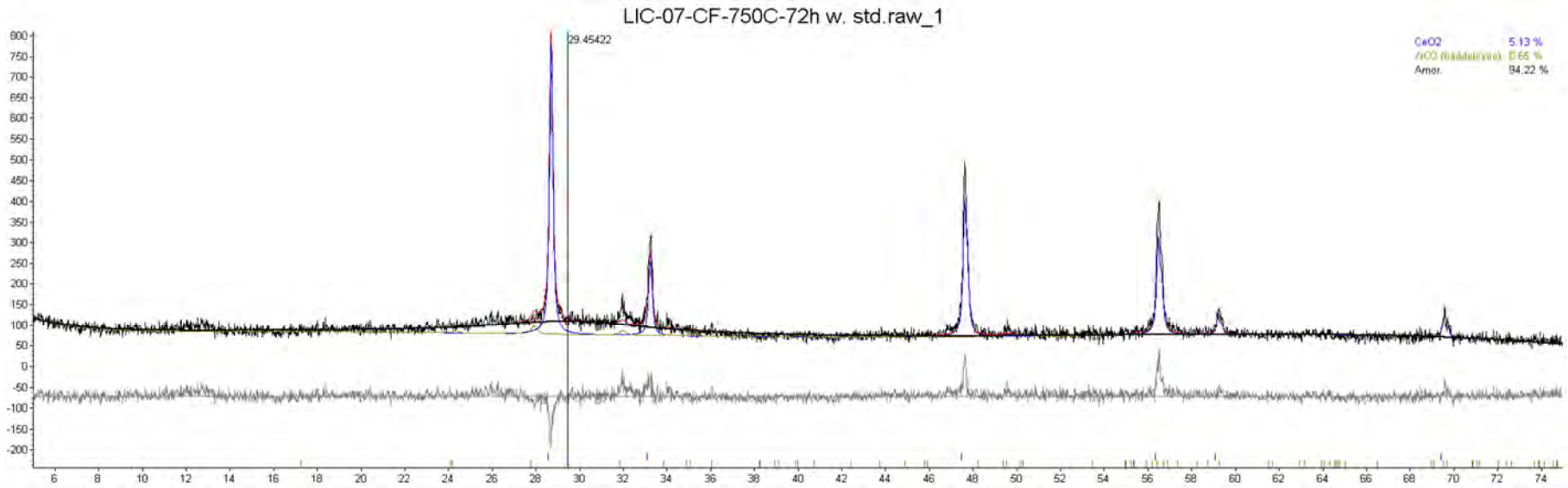

Figure D.22. XRD data for LIC-07-CF-750C-72h.

Table D.22. XRD data for LIC-07-CF-750C-72h.

Phase Name	Wt% of Spike	Wt% in Spiked Sample	Wt% in Original Sample
CeO_2	5.13	5.13	0.00
ZrO_2 (baddeleyite)	0.00	0.65	0.68

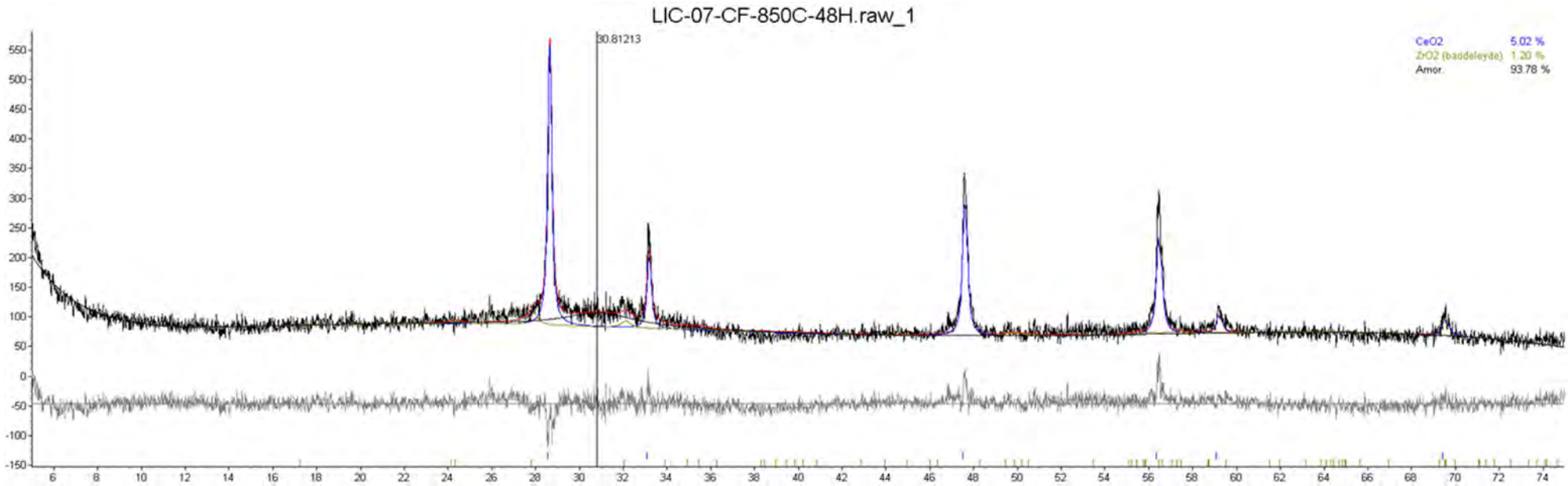

Figure D.23. XRD data for LIC-07-850C-48h.

Table D.23. XRD data for LIC-07-850C-48h.

Phase Name	Wt% of Spiked	Wt% in Spiked Sample	Wt% in Original Sample
CeO_2	5.02	5.02	0.00
ZrO_2 (baddeleyite)	0.00	1.20	1.27

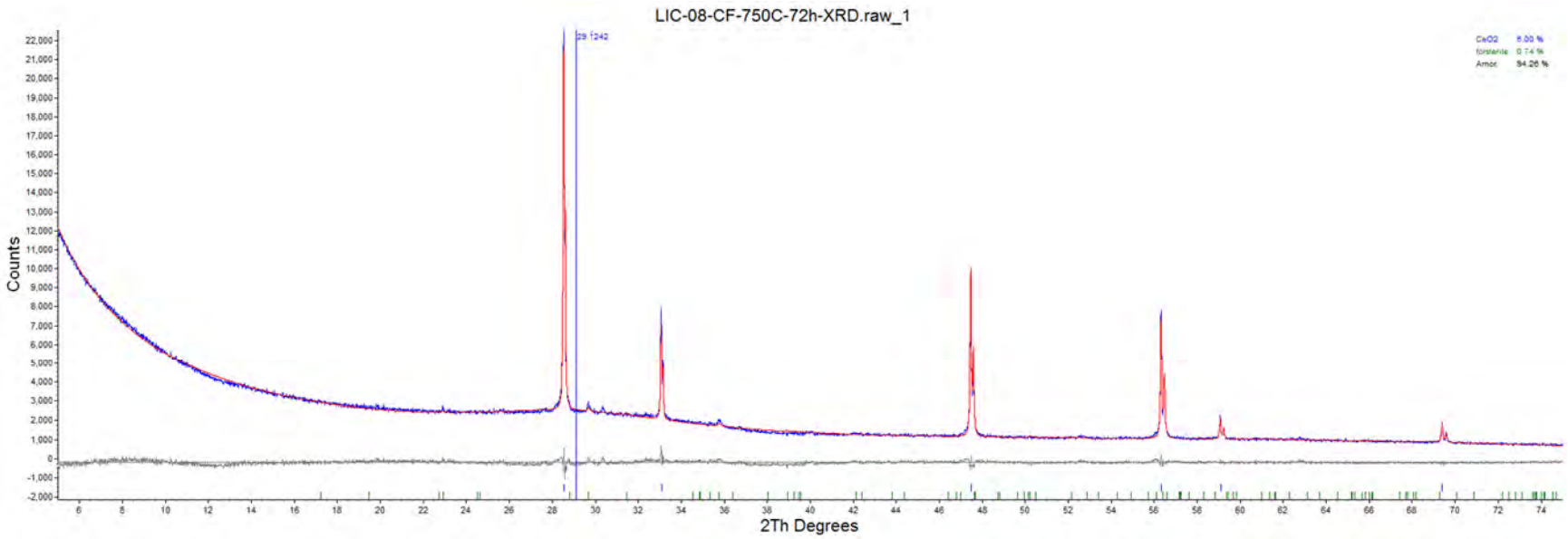

Figure D.24. XRD data for LIC-08-CF-750C-72h.

Table D.24. XRD data for LIC-08-CF-750C-72h.

Phase Name	Wt% of Spike	Wt% in Spiked Sample	Wt% in Original Sample
CeO_2	5.00	5.00	0.00
Forsterite	0.00	1.20	1.26
Diopside	0.00	3.19	3.35

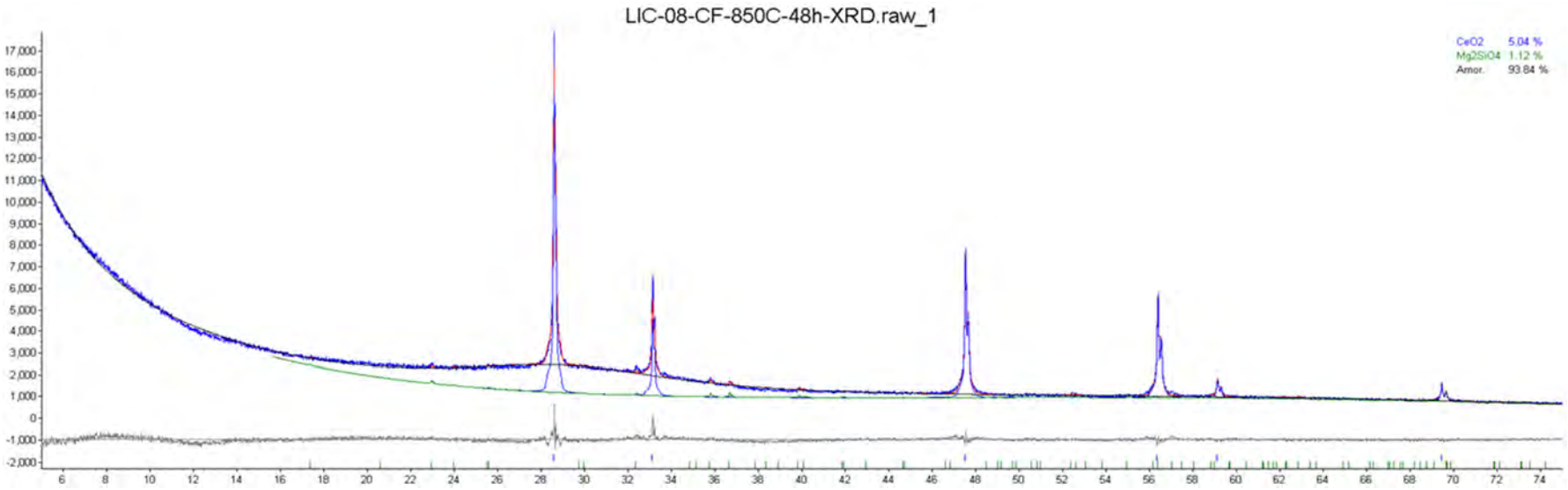

Figure D.25. XRD data for LIC-08-CF-850C-48h.

Table D.25. XRD data for LIC-08-CF-850C-48h.

Phase Name	Wt% of Spike	Wt% in Spiked Sample	Wt% in Original Sample
CeO_2	5.04	5.04	0.00
Forsterite	0.00	1.12	1.18

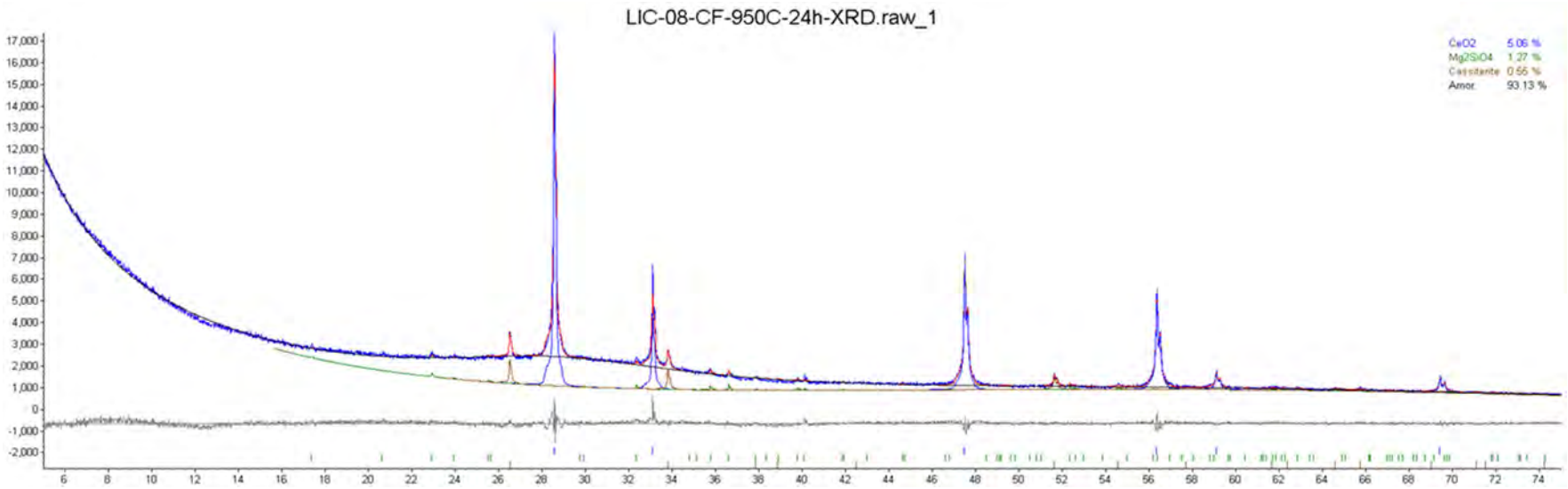

Figure D.26. XRD data for LIC-08-CF-950C-24h.

Table D.26. XRD data for LIC-08-CF-950C-24h.

Phase Name	Wt% of Spike	Wt% in Spiked Sample	Wt% in Original Sample
CeO_2	5.06	5.06	0.00
Forsterite	0.00	1.27	1.33
Cassiterite	0.00	0.55	0.58

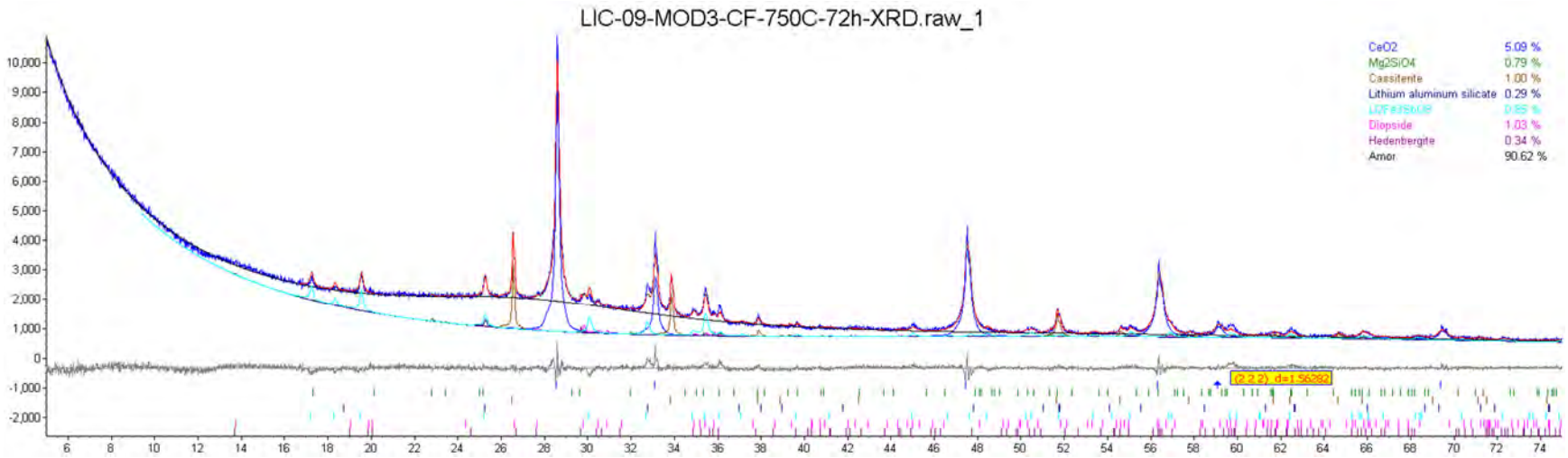

Figure D.27. XRD data for LIC-09-MOD3-CF-750C-72h.

Table D.27. XRD data for LIC-09-MOD3-CF-750C-72h.

Phase Name	Wt% of Spike	Wt% in Spiked Sample	Wt% in Original Sample
CeO_2	5.09	5.09	0.00
Forsterite	0.00	0.79	0.84
Cassiterite	0.00	1.00	1.05
Diopside	0.00	1.03	1.08
Hedenbergite	0.00	0.34	0.36
Lithium aluminum silicate	0.00	0.29	0.31
$Li_2Fe_3SbO_8$	0.00	0.85	0.89

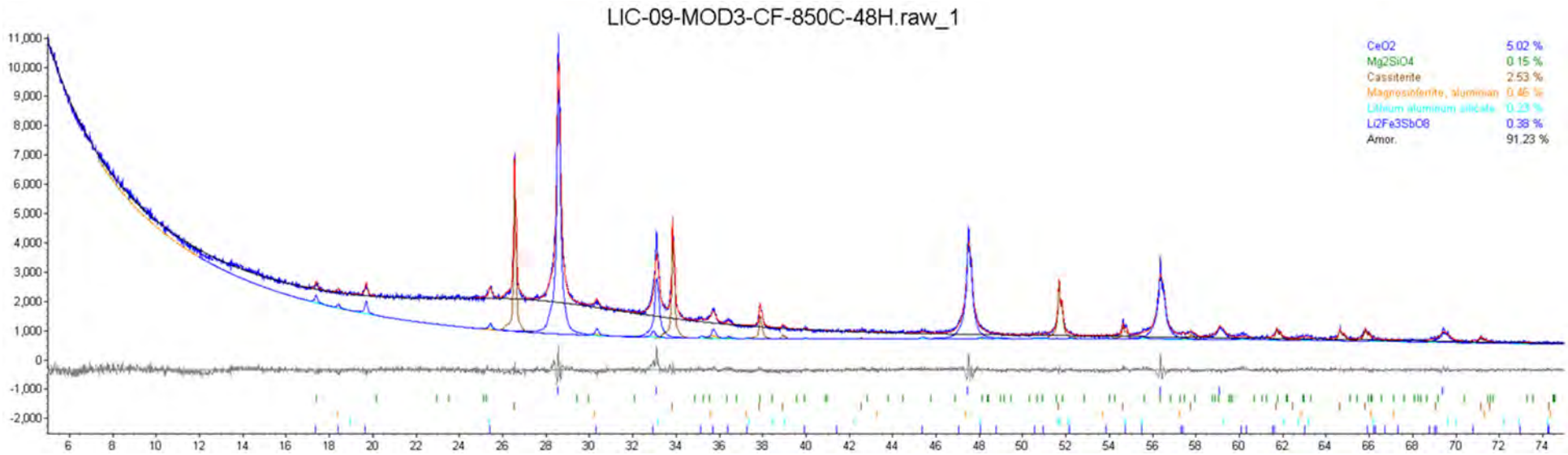

Figure D.28. XRD data for LIC-09-MOD3-CF-850C-48h.

Table D.28. XRD data for LIC-09-MOD3-CF-850C-48h.

Phase Name	Wt% of Spike	Wt% in Spiked Sample	Wt% in Original Sample
CeO_2	5.02	5.02	0.00
Forsterite	0.00	0.15	0.16
Cassiterite	0.00	2.53	2.66
Magnesioferrite, aluminian	0.00	0.46	0.48
Lithium aluminum silicate	0.00	0.23	0.25
$Li_2Fe_3SbO_8$	0.00	0.38	0.40

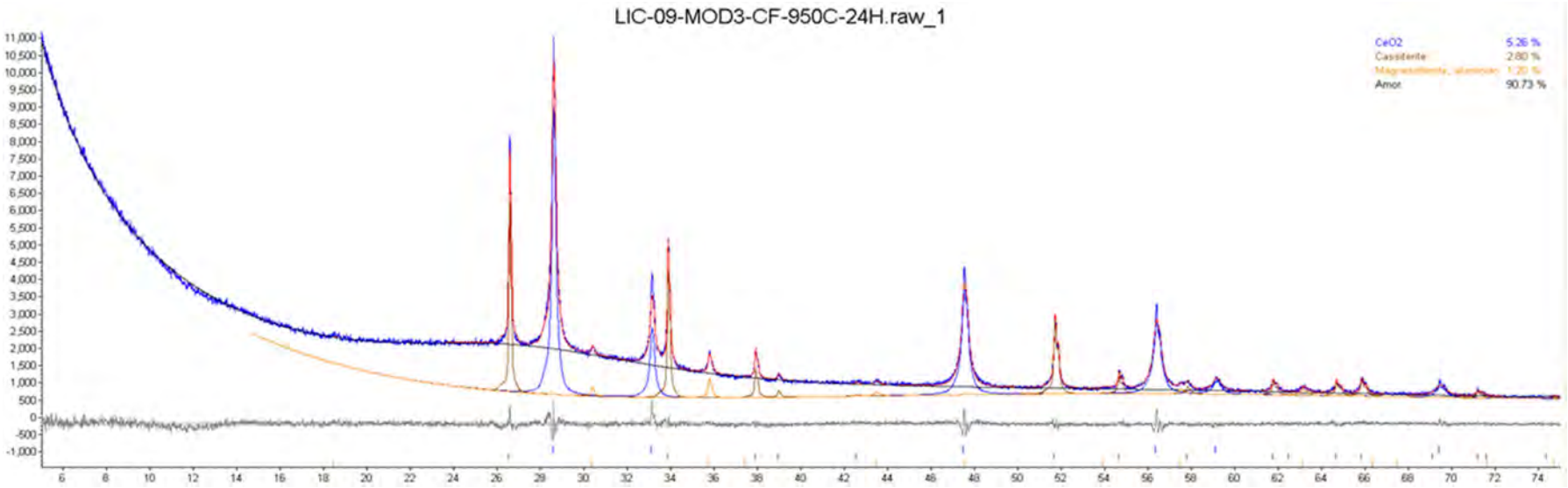

Figure D.29. XRD data for LIC-09-MOD3-CF-950C-24h.

Table D.29. XRD data for LIC-09-MOD3-CF-950C-24h.

Phase Name	Wt% of Spike	Wt% in Spiked Sample	Wt% in Original Sample
CeO_2	5.26	5.26	0.00
Cassiterite	0.00	2.80	2.96
Magnesioferrite, aluminian	0.00	1.20	1.27

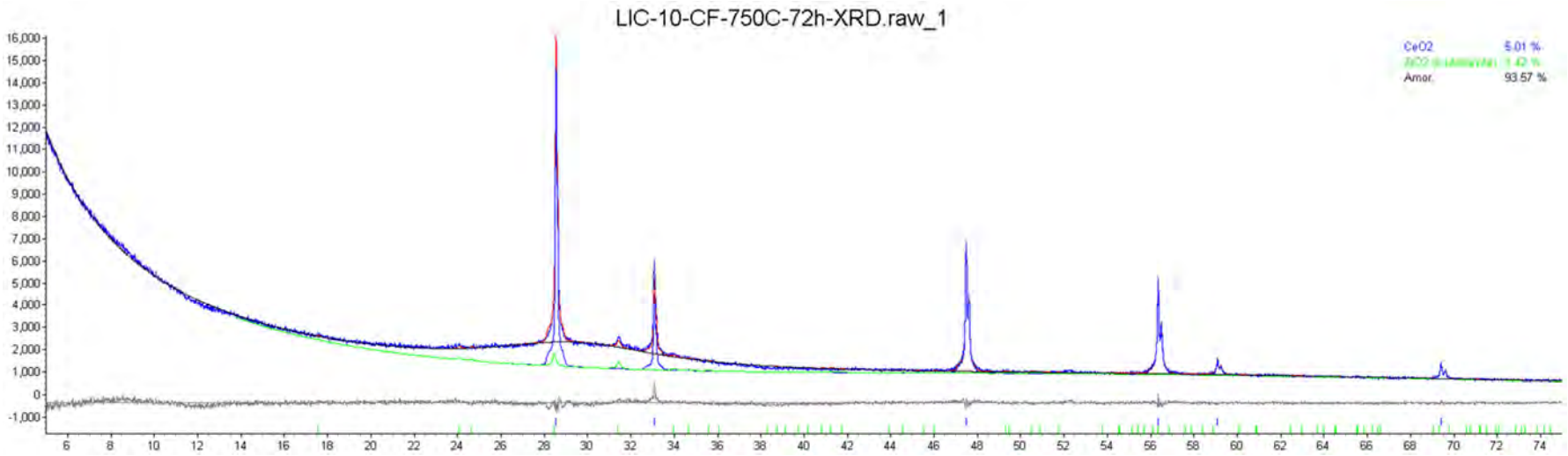

Figure D.30. XRD data for LIC-10-CF-750C-72h.

Table D.30. XRD data for LIC-10-CF-750C-72h.

Phase Name	Wt% of Spiked	Wt% in Spiked Sample	Wt% in Original Sample
CeO_2	5.01	5.01	0.00
ZrO_2 (baddeleyite)	0.00	1.42	1.50

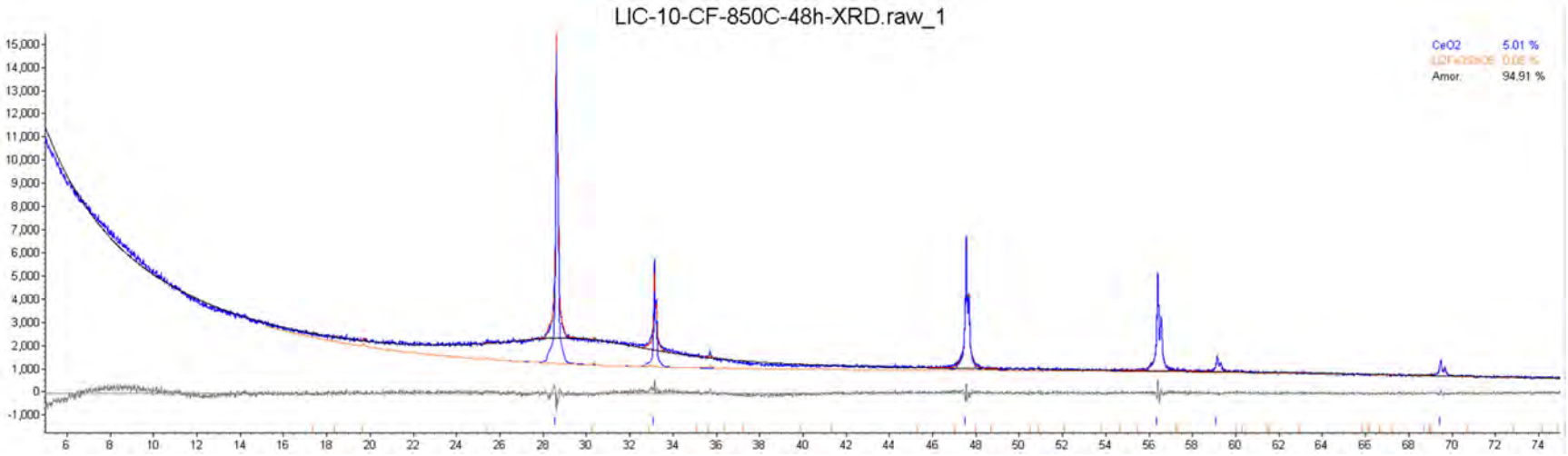

Figure D.31. XRD data for LIC-10-CF-850C-48h.

Table D.31. XRD data for LIC-10-CF-850C-48h.

Phase Name	Wt% of Spike	Wt% in Spiked Sample	Wt% in Original Sample
CeO_2	5.01	5.01	0.00
$Li_2Fe_3SbO_8$	0.00	0.08	0.09

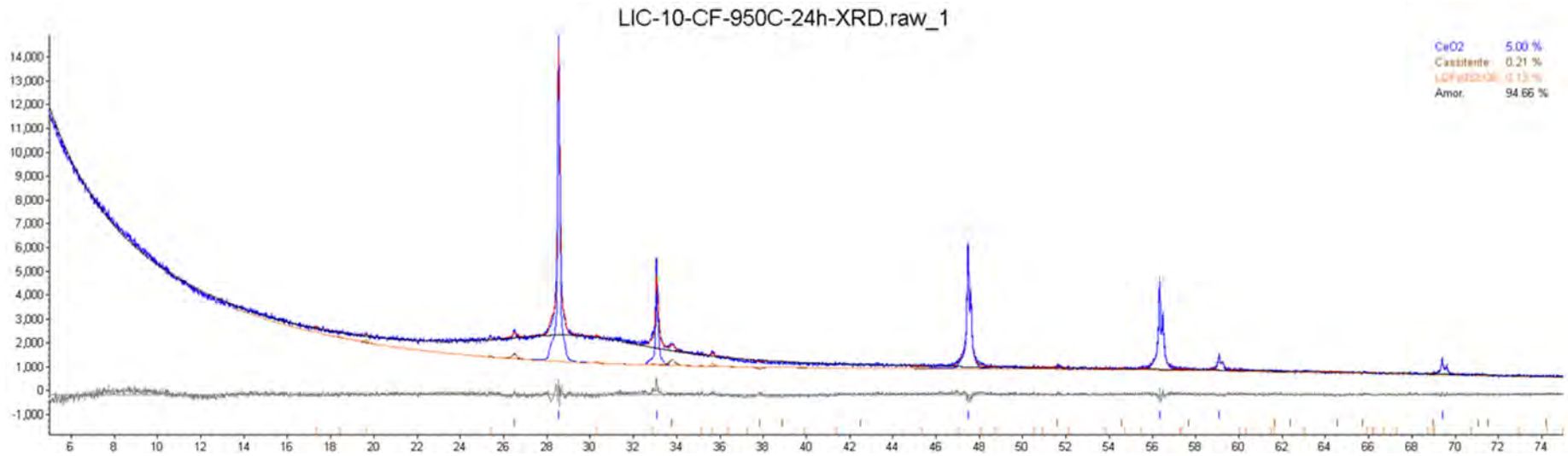

Figure D.32. XRD data for LIC-10-CF-950C-24h.

Table D.32. XRD data for LIC-10-CF-950C-24h.

Phase Name	Wt% of Spiked	Wt% in Spiked Sample	Wt% in Original Sample
CeO_2	5.00	5.00	0.00
Cassiterite	0.00	0.21	0.22
$Li_2Fe_3SbO_8$	0.00	0.13	0.13

Pacific Northwest National Laboratory

902 Battelle Boulevard
P.O. Box 999
Richland, WA 99354
1-888-375-PNNL (7665)

www.pnnl.gov